AD-A121 689 MONOLITHIC ZNO SAW STRUCTURES(U) PURDUE UNIV LAFAYETTE 1/1
IN SCHOOL OF ELECTRICAL ENGINEERING R L GUNSHOR ET AL.
01 JUN 82 AFOSR-TR-82-1005 AFOSR-81-0214

UNCLASSIFIED F/G 20/1 NL

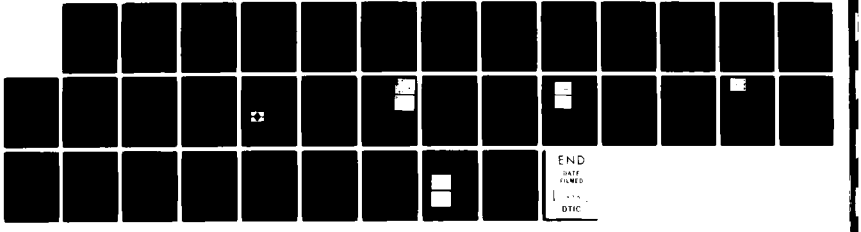

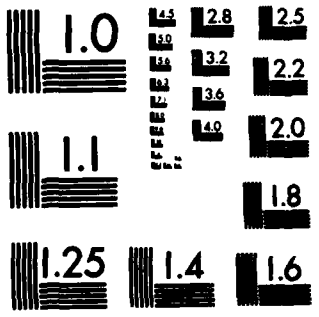

AFOSR-81-0214
Interim Scientific Report
1 June 1982

MONOLITHIC ZnO SAW STRUCTURES

R. L. Gunshor and R. F. Pierret

School of Electrical Engineering
Purdue University
West Lafayette, Indiana 47907

UNCLASSIFIED

SECURITY CLASSIFICATION OF THIS PAGE (When Data Entered)

REPORT DOCUMENTATION PAGE	READ INSTRUCTIONS BEFORE COMPLETING FORM
1. REPORT NUMBER: AFOSR-TR- 82-1005	2. GOVT ACCESSION NO. AD-A121 689 / 3. RECIPIENT'S CATALOG NUMBER
4. TITLE (and Subtitle): Monolithic ZnO SAW Structures	5. TYPE OF REPORT & PERIOD COVERED: Interim Scientific Report 1 May 81 to 30 April 82
	6. PERFORMING ORG. REPORT NUMBER
7. AUTHOR(s): R. L. Gunshor and R. F. Pierret	8. CONTRACT OR GRANT NUMBER(s): AFOSR-81-0214
9. PERFORMING ORGANIZATION NAME AND ADDRESS: School of Electrical Engineering, Purdue University, West Lafayette, IN 47907	10. PROGRAM ELEMENT, PROJECT, TASK AREA & WORK UNIT NUMBERS: 2306/B2 61102F
11. CONTROLLING OFFICE NAME AND ADDRESS: Air Force Office of Scientific Research/NE, Building 410, Bolling AFB, D.C. 20332	12. REPORT DATE: 1 June 82
	13. NUMBER OF PAGES: 35
14. MONITORING AGENCY NAME & ADDRESS (if different from Controlling Office): SAME	15. SECURITY CLASS. (of this report): UNCLASSIFIED
	15a. DECLASSIFICATION/DOWNGRADING SCHEDULE

16. DISTRIBUTION STATEMENT (of this Report)

Approved for public release; distribution unlimited.

17. DISTRIBUTION STATEMENT (of the abstract entered in Block 20, if different from Report)

SAME

18. SUPPLEMENTARY NOTES

N/A

19. KEY WORDS (Continue on reverse side if necessary and identify by block number)

Surface acoustic waves, ZnO, AlN piezoelectric devices, Microwave Acoustics, Electroacoustic convolvers, resonators

20. ABSTRACT (Continue on reverse side if necessary and identify by block number)

ZnO-on-silicon surface acoustic wave devices have been fabricated and tested. The first low temperature deposited AlN-on-silicon devices were reported. The performance of a high frequency transducer is discussed, and the operation of a new surface acoustic wave storage correlator, the induced junction correlator, is described.

DD FORM 1 JAN 73 1473 EDITION OF 1 NOV 65 IS OBSOLETE

UNCLASSIFIED

SECURITY CLASSIFICATION OF THIS PAGE (When Data Entered)

RESEARCH OBJECTIVES

Introduction

The role of monolithic surface acoustic wave (SAW) devices in performing the "real-time" analogue of various signal processing functions is by now widely accepted. Monolithic structures are intrinsically rugged, reproducible, and compatable with modern integrated circuit fabrication techniques. The emphasis of the research reported herein involves the evaluation of monolithic SAW structures and materials, with the research treating in large part modified structures and prototype device concepts.

Specific Tasks

1. An important consideration in the ultimate application of SAW signal processing devices to real systems is the available bandwidth. As a consequence, a major aspect of the project involves measures aimed at increasing the available bandwidth of monolithic SAW devices.

2. ZnO has proven to be an acceptable piezoelectric material for the implementation of monolithic, "on-silicon" device concepts. An alternate material, AlN, has been proposed as representing a possible improvement over, and replacement for ZnO. A portion of the project has been devoted to an examination of AlN for monolithic SAW applications.

3. It has been established that the electrical properties of the $Si-SiO_2$ subsystem are adversely affected by the ZnO deposition process. Methods for minimizing the effects of the sputtering damage are being examined and evaluated. Also, an instability related to the injection of electrons from the metal gate electrode into the underlying ZnO is observed upon applying a d.c. gate bias. We are seeking an understanding and constructive control or blocking of this injection process.

4. A wide range of analog linear and nonlinear signal processing functions are now feasible as a result of continuing developments in acoustic surface wave techniques. Under investigation are problems associated with achieving practical devices, such as correlators and resonators, using the monolithic technology.

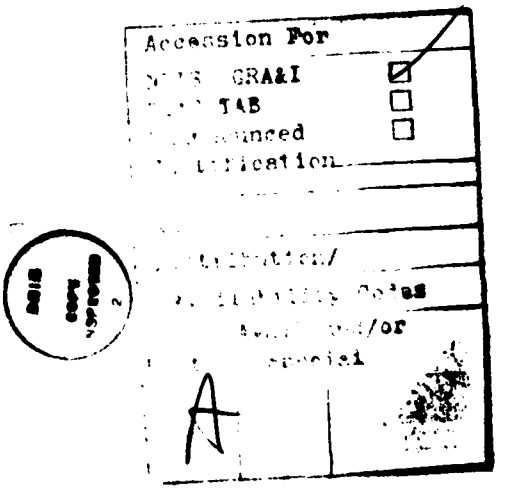

A. Bandwidth Considerations

The fractional bandwidth capability of monolithic SAW signal processing devices was significantly improved as a result of our previously reported work with Sezawa mode propagation. One development of the past year was the publication of the performance characteristics of a new transducer configuration for monolithic SAW devices. This transducer, called the separate comb transducer, is an adaptation of the single phase grating transducer that was earlier proven unsuccessful for transduction on single crystal substrates. We have demonstrated that the MZOS version of the single phase transducer performs quite well, and provides a significant advantage over the more conventional interdigital transducer when employed in the MZOS layered configuration. The improvement introduced by the separate comb transducer results in a relaxation of demands on the resolution requirements of the photolithographic process. A recent publication (Appendix A) describes how both increased operating frequencies and improved yield are expected when employing the separate comb transducer concept.

As a further demonstration of the increased SAW frequencies resulting from use of the separate comb transducer, we have demonstrated Rayleigh and Sezawa mode convolvers operating at the highest frequencies reported for MZOS structures. The Rayleigh mode convolver processed signals at 285 MHz, while the Sezawa mode device operated at 355 MHz. Complete details are provided by the reprint in Appendix B.

The concept of the coupling between Sezawa and Rayleigh modes relates to an additional development of the past year; the use of the multistrip coupler in the MZOS configuration. The primary motivation for an examination of the multistrip coupler structure originates from our continuing effort to enhance the performance of SAW convolvers. Along these lines we have been examining techniques for beamwidth compression (and hence increased power density and convolver efficiency), in the ZnO-SiO_2-Si configuration. One wide-band means of achieving acoustic beam compression employs a multistrip coupler (MSC) beam compressor. It is significant to note that heretofore MSC structures have been employed only on very high electromechanical coupling (high k^2) single crystal materials such as lithium niobate. Since we have previously demonstrated a high k^2 configuration employing the Sezawa mode, the opportunity for also implementing practical MSC structures in MZOS devices was apparent. During the past year we have fabricated a MSC beam-compressed device; the subsequent experiments exhibited an unexpected phenomenon. The results of these experiments were analyzed, and it was concluded the periodic MSC array not only coupled the acoustic beam to a parallel compressed track (the anticipated result), but also produced a narrow-band (and efficient) mode conversion from the input Sezawa mode energy to the Rayleigh mode. An unfortunate (or judicious, depending on newly envisioned applications) choice of MSC periodicity positioned the frequency of mode conversion near the center of the convolver passband. A subsequent series of experiments cofirmed the mode conversion hypothesis and further provided the design information required to either avoid or exploit the newly discovered

phenomenon, depending upon device objectives. A complete description of this work is included as reprints in Appendices C and D.

B. New Materials

Research performed during the past year has resulted in previously unreported developments involving monolithic SAW configurations based on an AlN film technology. By employing low substrate temperatures (<200°C) and reactive rf magnetron sputtering, we have succeeded in growing c-axis normal oriented piezoelectric films of AlN onto both SiO_2-Si and unoxidized silicon substrates. Some previous AlN work has involved low temperature deposition on saphire substrates or CVD deposition onto silicon at elevated substrate temperatures; the work reported here is the first demonstration of the performance of AlN-on-silicon SAW devices where low temperature fabrication was performed. (The interest in low temperature processing is related to compatability with integrated active devices on the silicon wafer.) The operation of AlN-on-silicon SAW delay lines, convolvers, and resonators is described in the reprints in Appendices E and F.

C. Charge Injection

During the past year we reported a ZnO-SiO_2-Si convolver in which the associated bias instability behavior was nearly eliminated. At the 1981 Ultrasonics Symposium we reported (reprint in Appendix G) the operation of a MZOS convolver in which the silicon surface bias potential can be rapidly changed (in both positive or negative directions) without evidence of significant hysteresis (bias instability) effects.

This stability was achieved through the use of a special annealing procedure. All previously reported MZOS signal processing devices have exhibited the bias instability behavior. It is especially interesting that the cited annealing procedure is effective for devices employing magnetron sputtered ZnO films, but not for diode sputtered films.

D. Induced Junction Storage Correlator

We have recently introduced a new device concept based directly on the charge injection phenomenon resulting from applying a dc bias to the gate. The new device utilizes charge stored in deep states at the ZnO-SiO_2 interface to induce discrete inverted regions at the silicon surface. The isolated inverted regions are found to accomplish the task previously performed by pn diode arrays in implementing storage correlator operation. Instead of information storage in diffused or Schottky diodes, here the correlator reference waveform is stored as variations in inversion layer charge in the array of inversion regions. The advantage of such a device configuration over more conventional diode correlators originates in the significantly simplified fabrication requirements, and the opportunities for electronic erasure. Details of device operation have been published, and a reprint is included as Appendix H.

E. SAW Resonators on Silicon

We have recently reported the development of the first VHF/UHF resonators on a silicon chip. It was found that such devices, constructed with available ZnO films, could exhibit Q values as high as

10,000 for these first test devices. Of even greater significance, however, was the demonstration of temperature stability comparable to ST quartz SAW resonators. The observed temperature stability resulted from the use of a compensating layer. It is important to emphasize that the compensating layer consists of a thermally grown silicon oxide. During the past year we have emphasized the elimination of the effects of transverse modes on the response characteristic of the resonator, the optimization of reflection grating parameters, and the examination of aging characteristics. (The aging data was obtained in collaboration with North American Rockwell.) Details of the resonator work will appear in future publications.

PUBLICATIONS

M. R. Melloch, R. L. Gunshor, and R. F. Pierret, "Sezawa to Rayleigh Mode Conversion in the ZnO-on-Si Surface Acoustic Wave Configuration," Applied Physics Letters, 39, 476 (1981).

M. R. Melloch, R. L. Gunshor, and R. F. Pierret, "Conversion of Sezawa to Rayleigh Waves in the ZnO-SiO_2-Si Configuration," Proceedings of 1981 IEEE Ultrasonics Symposium, p. 765.

L. G. Pearce, R. L. Gunshor, and R. F. Pierret, "Sputtered Aluminum Nitride on Silicon for SAW Device Applications," Proceedings of 1981 IEEE Ultrasonics Symposium, p. 381.

R. D. Cherne, M. R. Melloch, R. L. Gunshor, and R. F. Pierret, "Bias Stable Zinc Oxide-on-Silicon Surface Acoustic Wave Devices," Proceedings of 1981 IEEE Ultrasonics Symposium, p. 780.

L. G. Pearce, R. L. Gunshor, and R. F. Pierret, "Aluminum Nitride on Silicon Surface Acoustic Wave Devices," Applied Physics Letters, 39, 878 (1981).

M. R. Melloch, R. L. Gunshor, and R. F. Pierret, "High Frequency ZnO-SiO_2-Si Surface Acoustic Wave Convolvers," Electronics Letters, 17, 827 (1981).

M. R. Melloch, R. L. Gunshor, and R. F. Pierret, "Single-Phase and Balanced Separate Comb Transducer Configurations in a ZnO/Si SAW Structure," IEEE Transactions on Sonics and Ultrasonics, SU-29, 55 (1982).

K. C.-K. Weng, R. L. Gunshor, and R. F. Pierret, "Induced Junction Monolithic Zinc Oxide-on-Silicon Storage Correlator," Applied Physics Letters, 40, 71 (1982).

PERSONNEL

Robert L. Gunshor, Professor of Electrical Engineering

Robert F. Pierret, Professor of Electrical Engineering

Ken Weng, Graduate Research Assistant

Steve J. Martin, Graduate Research Assistant

Mike R. Melloch, Graduate Research Assistant

Larry Pearce, Graduate Research Assistant

Jeff A. Shields, Graduate Research Assistant

Gary Bernstein, Graduate Research Assistant

Tim Miller, Technician

Single-Phase and Balanced Separate Comb Transducer Configurations in a ZnO/Si SAW Structure

M. R. MEILOCH, R. L. GUNSHOR, SENIOR MEMBER, IEEE, AND R. F. PIERRET

Abstract—The operating frequency corresponding to a given photolithographic limit can be doubled by employing a single-phase transducer configuration instead of the conventional interdigital transducer (IDT) configuration. It is found that the signal level due to direct coupling in the single-phase structure is reduced by employing a balanced transducer configuration using two single-phase delay lines in parallel. Both Rayleigh and Sezawa mode operations in the ZnO-SiO_2-Si structure are described.

I. Introduction

The interdigital transducer (IDT) [1] is the most efficient means of exciting and detecting surface acoustic waves (SAW) on piezoelectric media. It consists of a series of metal strips where alternate strips are interconnected as shown in Fig. 1(a). The upper limit on the operating frequency of a SAW device is determined by the capability of the photolithographic technique being used to define the interdigital transducer. A configuration employing a two-layer transducer on lithium niobate has been used to double the frequency range for $LiNbO_3$ SAW devices [2]. Herein we describe a technique for doubling the operating frequency for use in the ZnO-on-silicon layered device configuration.

The proposed transducer structure is shown in Fig. 1(b) and is referred to as the "single-phase" structure [3]. The metal widths and spacings for the single-phase structure are $\lambda/2$ (where λ = wavelength of the SAW) while the metal widths and spacings for the conventional IDT structure are $\lambda/4$. Thus for a given photolithographic limit, one can obtain twice the operating frequency with the single-phase structure as opposed to the IDT structure. It is important to note that a single-phase transducer in the form of a grating [4], as shown in Fig. 1(c), will improve device yields. The yields improve because electrical shorts between fingers or a break in a finger will alter just a small portion of the transducer's active region.

II. Device Structures and Performance

A Rayleigh mode single-phase transducer delay line has been constructed in the ZnO-SiO_2-Si configuration. The Rayleigh waves propagate in the (100) direction on a (100)-cut 7-$\Omega \cdot$ cm n-silicon substrate. A 0.12-μm SiO_2 film thermally grown on the silicon substrate is covered with a 2.6-μm thick ZnO film deposited by radio frequency (RF) sputtering. The transducers consist of 20 aluminum fingers of equal width and gap (22.9 μm) located on top of the ZnO, with an aluminum underlay at the ZnO-SiO_2 interface. The SAW acoustic beamwidth is 1 mm, and the center-to-center transducer spacing is 12.7 mm. Both input and output transducers were tuned with series inductors, and there is a convolver gate [5] located between the transducers.

Manuscript received March 24, 1981; revised July 14, 1981. This work was supported by the Air Force Office of Scientific Research under Grant No. AFOSR-77-3304, National Science Foundation Grant No. ENG 76-11229, and NSF-MRL Grant No. DMR 77-23798.

The authors are with the School of Electrical Engineering, Purdue University, West Lafayette, IN 47907.

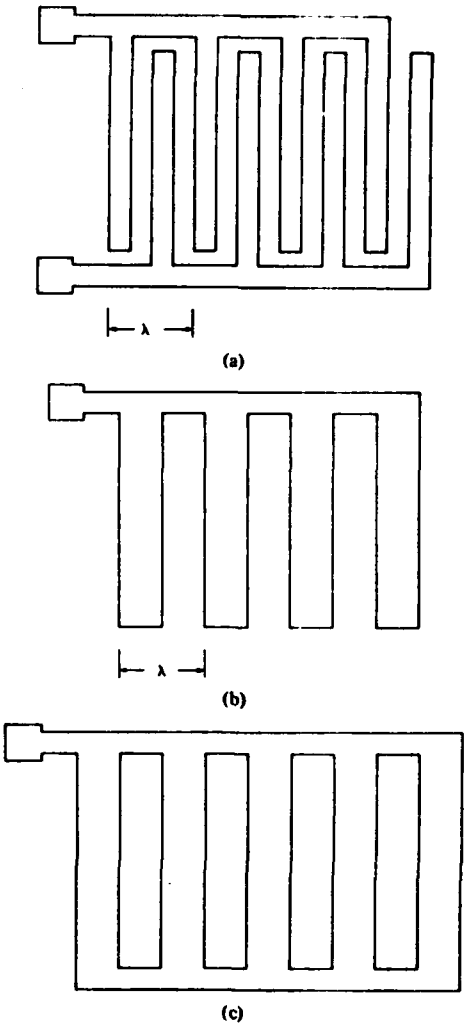

Fig. 1. (a) Conventional interdigital transducer configuration. (b) Single-phase transducer configuration. (c) Single-phase grating transducer configuration.

Fig. 2 shows the two-port insertion loss for the Rayleigh device plotted as a function of frequency. The insertion loss at the synchronous frequency, f_0 = 94 MHz, is 25 dB. This loss value is comparable to that achieved with other monolithic zinc-oxide-on-silicon (MZOS) Rayleigh delay lines [6]–[9]. However, it was found that the background signal level, due to direct electromagnetic coupling between the single-phase transducers, is only 25 dB below the response peak. In the IDT structure, this direct coupling is often reduced by means of a balanced excitation, which is implemented by driving both combs with signals that have a 180° phase offset. When using the single-phase structure, we have found that one can make use of a balanced drive by placing two single-phase delay lines in parallel as shown in Fig. 3; we will refer to this arrangement as the separate comb configuration.

In Fig. 4 the two-port insertion loss for a balanced separate

0018-9537/82/0100-0055$00.75

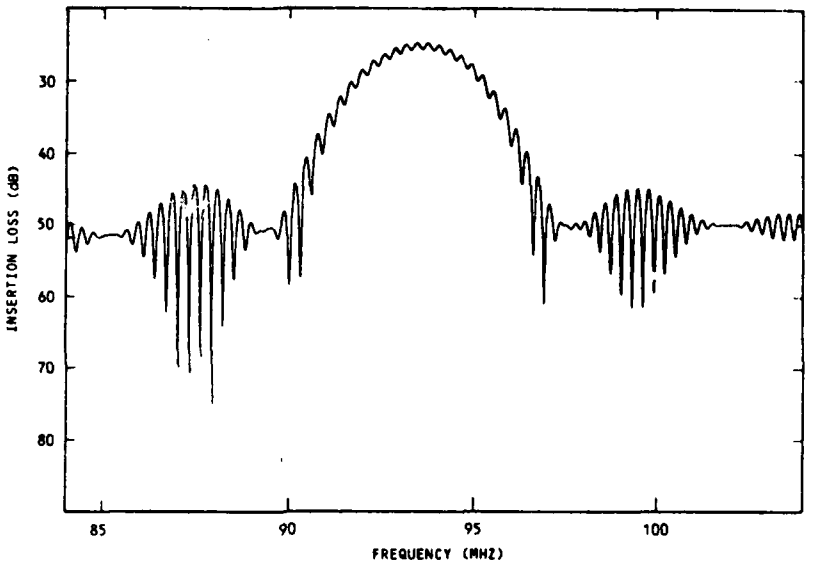

Fig. 2. Frequency response of single-phase transducer Rayleigh device.

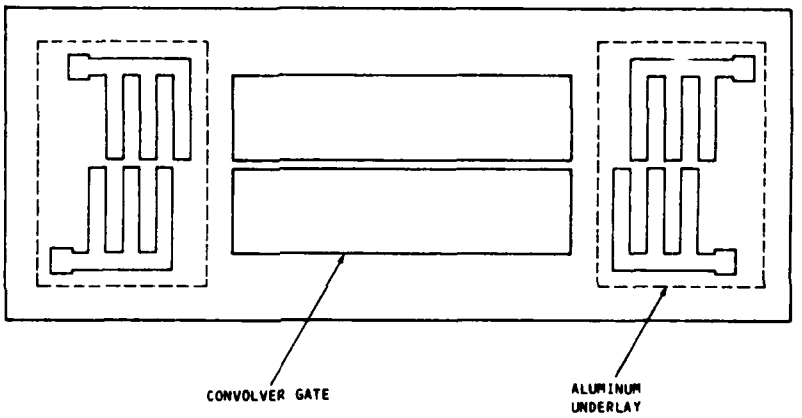

Fig. 3. Separate comb transducer device configuration.

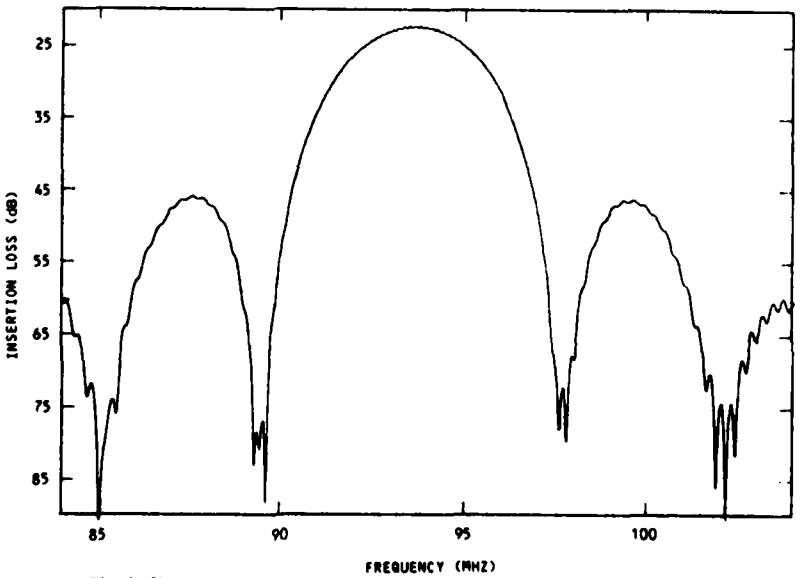

Fig. 4. Frequency response of separate comb transducer Rayleigh device.

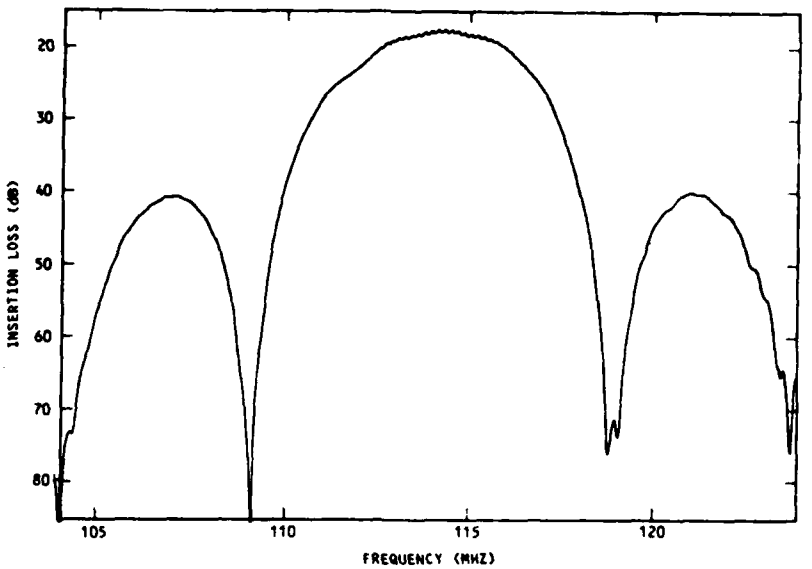

Fig. 5. Frequency response of separate comb transducer Sezawa device.

comb Rayleigh device is shown. All the parameters are the same as the previously described Rayleigh device except that the beamwidth is now 2 mm and there are two convolver gates, one between each half of the transducers. The synchronous insertion loss is 22 dB, and the background noise level is now 60 dB below the peak transduction. It should be noted that this structure is similar in complexity to a convolver configuration used to obtain self-convolution suppression [10].

In addition to the Rayleigh device, a Sezawa mode balanced separate comb transducer delay line was also constructed. Here the parameters are the same as for the balanced separate comb Rayleigh device except that the ZnO film is now 10-μm thick and is deposited by RF magnetron sputtering [11].

The two-port insertion loss for the Sezawa device is plotted as a function of frequency in Fig. 5. The insertion loss at the synchronous frequency, $f_0 = 114.5$ MHz, is 18 dB, a value comparable with other MZOS Sezawa delay lines [12]–[13].

III. Discussion

The comparison of interdigital transducers in the MZOS structure under balanced and unbalanced excitation has been examined by Webb and Banks [14]. The single-phase and separate comb transducers can be compared to the IDT by using the normal mode approach described by Kino and Wagers [15]. For the MZOS structure the radiation resistance R_a and the static capacitance C_T for a balanced drive IDT are

$$R_a = \frac{4}{\omega l}\left(\frac{\sin\frac{\pi d}{\lambda}}{\frac{\pi d}{\lambda}}\right)^2 \cdot \frac{1}{\left[\epsilon_0 + (\epsilon_{xx}\epsilon_{zz})^{1/2}\coth\left(\left(\frac{2\pi}{\lambda}\right)\left(\frac{\epsilon_{xx}}{\epsilon_{zz}}\right)^{1/2} H\right)\right]}\frac{\Delta v}{v} \quad (1)$$

$$C_T = N\pi l\left[4\sum_{m=0}^{\infty}\left(\frac{\sin|(2m+1)\pi d/\lambda|}{(2m+1)\pi d/\lambda}\right)^2 \times \frac{1}{(2m+1)\left[\epsilon_0 + (\epsilon_{xx}\epsilon_{zz})^{1/2}\coth\left[2\pi\frac{(2m+1)}{\lambda}\left(\frac{\epsilon_{xx}}{\epsilon_{zz}}\right)^{1/2} H\right]\right]}\right]^1 \quad (2)$$

where

N	number of finger pairs,
d	finger width,
l	finger length,
v	wave velocity,
Δv	perturbation in wave velocity,
H	ZnO thickness,
λ	acoustic wavelength,
ω	synchronous frequency,
$\epsilon_{xx}, \epsilon_{zz}$	permittivities for ZnO.

The normal mode approach applied to the balanced separate comb transducer for evaluation of the radiation resistance and static capacitance gave the same results as (1) and (2).

Equations (1) and (2) can be used to make a comparison between a balanced separate comb transducer having N fingers in each parallel half of the transducer and an IDT having N finger pairs and operated with balanced drive. In both examples, the finger width to spacing ratio is taken as unity, and they have the same beamwidth. It is found that the balanced separate comb transducer has the same radiation resistance and static capacitance as the IDT structure using balanced excitation. Therefore the electrical fractional bandwidth, given by $\Delta f/f_0 = 2\pi f_0 C_T R_a$, is the same for the balanced separate comb and balanced IDT structures.

The radiation resistance of the previously described balanced separate comb Rayleigh device is measured to be 16.5 Ω. The value of R_a obtained from (1) is 19.4 Ω. The measured static capacitance is 8 pF, while a value of 9.5 pF was obtained from (2).

Using the normal mode approach, the radiation resistance and static capacitance for the single-phase transducer and the IDT driven unbalanced are

$$R_a = \frac{1}{\omega l}\left(\frac{\sin\frac{\pi d}{\lambda}}{\frac{\pi d}{\lambda}}\right)^2 \frac{1}{\left[\epsilon_0 + (\epsilon_{xx}\epsilon_{zz})^{1/2}\coth\left(\frac{2\pi}{\lambda}\left(\frac{\epsilon_{xx}}{\epsilon_{zz}}\right)^{1/2} H\right)\right]}\frac{\Delta v}{v} \quad (3)$$

$$C_T = \pi N l \left[\frac{\pi H}{\lambda \epsilon_{zz}} + \sum_{m=1}^{\infty} \left(\frac{\sin \frac{m\pi d}{\lambda}}{\frac{m\pi d}{\lambda}} \right)^2 \cdot \frac{1}{m \left[\epsilon_0 + (\epsilon_{xx}\epsilon_{zz})^{1/2} \coth \left(m \frac{2\pi}{\lambda} \left(\frac{\epsilon_{xx}}{\epsilon_{zz}} \right)^{1/2} H \right) \right]} \right]^{-1}. \quad (4)$$

Using (3) and (4) a comparison can be made between a single-phase transducer of N fingers and an IDT of N finger pairs that is driven unbalanced. The ratio of finger width to spacing was taken as unity for both transducers, and they have the same beamwidth. For the single-phase structure, the radiation resistance is found to be one-half and the static capacitance is twice that of the unbalanced IDT structure. Therefore, the electrical fractional bandwidth is the same for the single-phase structure and the IDT structure with unbalanced drive.

The radiation resistance of the previously described single-phase Rayleigh device is measured to be 4 Ω. The value of R_a obtained from (3) is 4.8 Ω. The measured static capacitance is 14 pF, while a value of 17.5 pF is obtained from (4).

IV. Conclusion

We have demonstrated a technique for doubling the operating frequency for both MZOS Rayleigh and Sezawa mode transducers without an increase in conversion loss or in the amount of direct coupling. In addition, for devices constructed for a particular frequency, the device yields will be improved with use of the single-phase grating structure. The expected improvement is due not only to increased metal widths and spacings, but also because shorts between transducer fingers or a break in a finger should have little effect on the performance of the transducer.

Acknowledgment

This work was supported by the Air Force Office of Scientific Research under Grant No. AFOSR-77-3304, National Science Foundation Grant No. ENG 76-11229, and NSF-MRL Grant No. DMR 77-23798.

References

[1] R. M. White and F. W. Volter, "Direct piezoelectric coupling to surface elastic waves," *Appl. Phys. Lett.*, vol. 26, pp. 314–316, 1965.
[2] H. Harada and R. L. Gunshor, "Two-layer interdigital transducer for acoustic-surface-wave devices," *Electron. Lett.*, vol. 12, pp. 82–84, 1976.
[3] L. A. Coldren, "Effect of bias field in a zinc-oxide-on-silicon acoustic convolver," *Appl. Phys. Lett.*, vol. 25, pp. 473–475, 1974.
[4] R. M. Artz, E. Salzmann, and K. Dransfeld, "Elastic surface waves in quartz at 316 MHz," *Appl. Phys. Lett.*, vol. 10, pp. 165–167, 1967.
[5] M. Luukkala and G. S. Kino, "Convolution and time inversion using parametric interactions of acoustic surface waves," *Appl. Phys. Lett*, vol. 18, pp. 393–394, 1971.
[6] B. T. Khuri-Yakub and G. S. Kino, "A monolithic zinc-oxide-on-silicon convolver," *Appl. Phys. Lett.*, vol. 25, pp. 188–190, 1974.
[7] K. L. Davis, "Storage of optical patterns in an zinc-oxide-on-silicon surface wave convolver," *Appl. Phys. Lett.*, vol. 26, pp. 143–145, 1975.
[8] J. K. Elliott, R. L. Gunshor, R. F. Pierret, and K. L. Davis, "Zinc oxide-silicon monolithic acoustic surface wave optical image scanner," *Appl. Phys. Lett.*, vol. 27, pp. 179–181, 1975.
[9] M. R. Melloch, R. L. Gunshor, C. L. Liu, and R. F. Pierret, "Interface transduction in the ZnO-SiO_2-Si surface acoustic wave device configuration," *Appl. Phys. Lett.*, vol. 37, pp. 147–150, 1980.
[10] I. Yao, "High performance elastic convolver with parabolic horns," in *Proc. 1980 Ultrason. Symp.*, pp. 37–42.
[11] T. Shiosaki, "High-speed fabrication of high-quality sputtered ZnO thin-films for bulk and surface wave applications," in *Proc. 1978 Ultrason. Symp.*, pp. 100–110.
[12] J. K. Elliott, R. L. Gunshor, R. F. Pierret, and A. R. Day, "A wideband SAW convolver utilizing Sezawa waves in the metal-ZnO-SiO_2-Si configuration," *Appl. Phys. Lett.*, vol. 32, pp. 515–516, 1978.
[13] F. C. Lo, R. L. Gunshor, and R. F. Pierret, "Monolithic (ZnO) Sezawa-mode pn-diode-array memory correlator," *Appl. Phys. Lett.*, vol. 34, pp. 725–726, 1979.
[14] D. C. Webb and C. Banks, "Surface-acoustic-wave excitation in the zinc oxide-on-silicon configuration," in *Proc. 1978 Ultrason. Symp.*, pp. 697–700.
[15] G. S. Kino and R. S. Wagers, "Theory of interdigital couplers on nonpiezoelectric substrates," *J. Appl. Phys.*, vol. 44, pp. 1480–1488, 1973.

evaporated AuZn and AuGe, respectively. The diameter of the active region was 100 μm.

A guard ring plays the most important role in determining avalanche gains in planar APDs. In preliminary studies using InP epitaxial wafers, it was found that the Be-implanted layer forms a linearly graded junction and its breakdown voltage is greater than that of a Cd-diffused abrupt junction. The edge breakdown, however, cannot be prevented solely by this linearly graded junction because of a curvature effect by the shallow junction (2 μm). Therefore, as seen in Fig. 1, the upper n^--InP layer was prepared to avoid the edge breakdown. This two-step guard ring produced a difference in the breakdown voltages between the guard ring and active regions. The breakdown voltage of the guard ring was 110 V. After the Cd-diffusion, the avalanche breakdown occurred at about 89 V (see Fig. 3). The difference was more than 20 V.

The guard ring effect was studied by a spot-scanned photoresponse at a wavelength of 1·3 μm (InGaAsP laser diode). The results obtained are shown in Fig. 2. The spot size was about 10 μm. The photoresponse in the active region was much greater than in the guard ring region. An effective guard ring can be recognised in this Figure. The multiplication characteristics are shown as a function of the bias voltage in Fig. 3. The photoresponse increased rapidly at about 25 V, corresponding to the punchthrough of the depletion region from the InP into the InGaAsP. In the voltage region of 25–40 V, the noticable increase of the photoresponse was not obtained. This indicates that the multiplication factor of this voltage region can be defined to be unity. The maximum avalanche gain was 110 at an initial photocurrent of 0·35 μA and at 1·3 μm. The quantum efficiency at 1·3 μm was about 50% at 35 V without an anti-reflection coating. A value of about 70% is expected by applying an optimum coating. The dark current of the diode is also shown in Fig. 3. The value was 20 nA at 90% of the breakdown voltage.

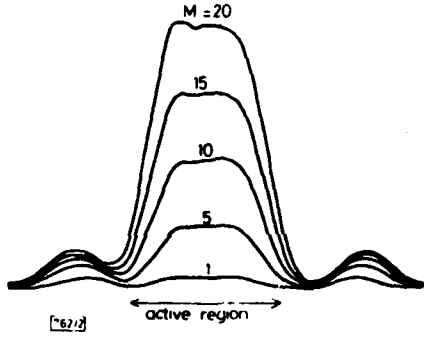

Fig. 2 *Spot-scanned photoresponse across centre of diode*
λ = 1·3 μm

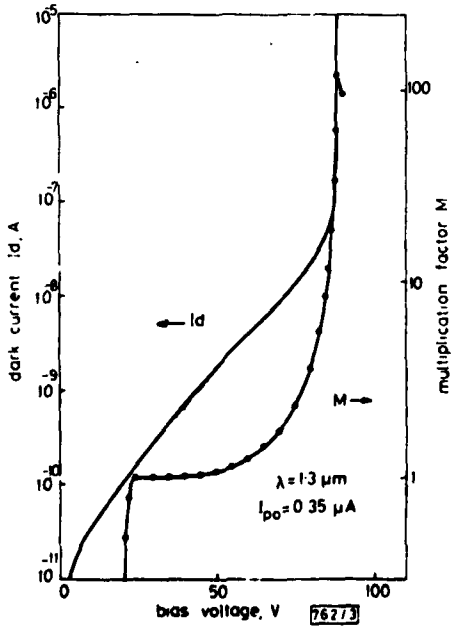

Fig. 3 *Dark current and multiplication factors of diode*

In summary, an InP/InGaAsP planar APD operating at a wavelength of 1·3 μm has for the first time been fabricated by using Be implantation and a difference of impurity concentrations between two InP layers. A sufficient guard ring effect was demonstrated by a spot-scanned photoresponse, and an avalanche gain of 110 was obtained at an initial photocurrent of 0·35 μA.

We would like to thank T. Ikegami and T. Kimura in NTT for their continuing guidance and encouragement. We would also like to acknowledge useful discussions with T. Sakurai, K. Akita, T. Hashimoto, T. Mikawa and K. Yasuda.

T. SHIRAI
F. OSAKA
S. YAMASAKI
K. NAKAJIMA
T. KANEDA

Fujitsu Laboratories Ltd.
1015 Kamikodanaka, Nakaharaku, Kawasaki, Japan

16th September 1981

References

1 DIADUIK, V., GROVES, S. H., and HURWITZ, C. E.: 'Avalanche multiplication and noise characteristics of low dark current GaInAsP/InP avalanche photodetectors', *Appl. Phys. Lett.*, 1980, 37, pp. 807–810

2 SUSA, N., NAKAGOME, H., MIKAMI, O., ANDO, H., and KANBE, H.: 'New InGaAs/InP avalanche photodiode structure for 1·0–1·6 μm wavelength region', *IEEE J. Quantum Electron.*, 1980, QE-16, pp. 868–870

3 OSAKA, F., NAKAJIMA, K., KANEDA, T., and SAKURAI, T.: 'InP/InGaAsP avalanche photodiodes with new guard ring structure', *Electron. Lett.*, 1980, 16, pp. 716–717

0013-5194/81/220826-02$1.50/0

HIGH FREQUENCY ZnO-SiO_2-Si SURFACE ACOUSTIC WAVE CONVOLVERS

Indexing terms: Surface acoustic waves, Convolvers

The separate comb grating transducer configuration is used in the fabrication of high frequency convolvers in the metal-ZnO-SiO_2-Si surface acoustic wave device structure. A Rayleigh convolver with an operating frequency of 285 MHz and a Sezawa convolver with an operating frequency of 355 MHz are reported.

The use of the separate comb transducer configuration[1] in the metal-ZnO-SiO_2-Si (MZOS) surface acoustic wave (SAW) configuration enables one to double the operating frequency for a given photolithographic capability. The increase is due to the fact that the metal widths and spacings are $\lambda/2$ (where λ = wavelength of the SAW) for the separate comb configuration, while the metal widths and spacings for the conventional interdigital transducer are $\lambda/4$. We have employed the separate comb grating transducer (SCGT) in the construction of high frequency Rayleigh and Sezawa convolvers in the MZOS structure which are described in this letter.

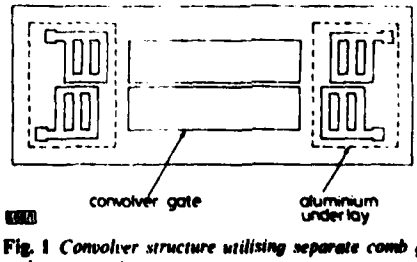

Fig. 1 *Convolver structure utilising separate comb grating transducers and two convolver gates*

structure is depicted in Fig. 1. Two convolver gates are shown, one between each half of the SCGT. A configuration of this type, with an appropriate shift in transducer position, can be used to obtain self-convolution suppression.[2] The devices were fabricated on (100)-cut 7 Ωcm *n*-silicon substrates and the SAW propagation was in the ⟨100⟩ direction. A 0·12 μm SiO_2 film was thermally grown on the silicon substrate and then 0·6 μm or 2·8 μm of ZnO was deposited by RF sputtering for the Rayleigh and Sezawa devices, respectively. The SCGT consisted of 20 aluminium fingers in each half of the transducer, which was designed for a wavelength of 15·24 μm, located on top of the ZnO, with an aluminium underlay at the ZnO-SiO_2 interface. The SAW beamwidth was 0·15 cm and the centre-to-centre transducer spacing was 1·27 cm. The transducers were driven balanced and the convolution output was taken from both convolver gates.

The fabricated Rayleigh convolver had a synchronous frequency of $f_0 = 285$ MHz and a two port insertion loss of 36 dB. This synchronous frequency is more than 100 MHz higher than any previously reported MZOS Rayleigh convolver.[3,4] A maximum convolution efficiency[5] of $F_T = -89$ dBm was obtained and the convolution efficiency and insertion loss against gate bias are shown in Fig. 2. (A stationary state was established after strong illumination at each bias value,[6] while the actual convolution efficiency and insertion loss measurements were taken in the dark.) The convolution output at 570 MHz for two RF modulated rectangular pulses is shown in Fig. 3.

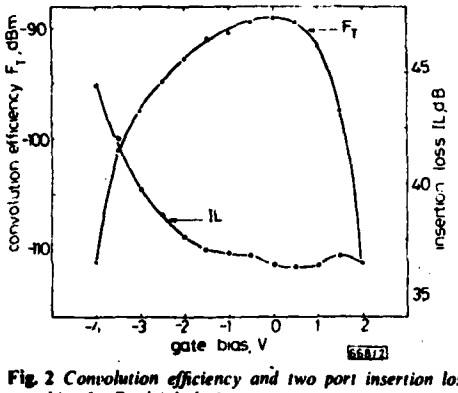

Fig. 2 *Convolution efficiency and two port insertion loss against DC gate bias for Rayleigh device*

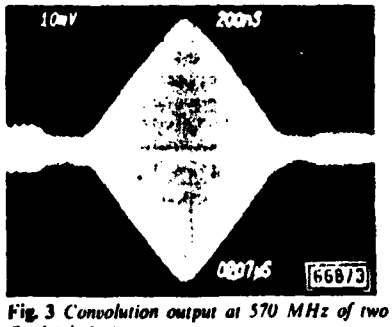

Fig. 3 *Convolution output at 570 MHz of two rectangular pulses for Rayleigh device*

Horizontal axis: 200 ns/div.

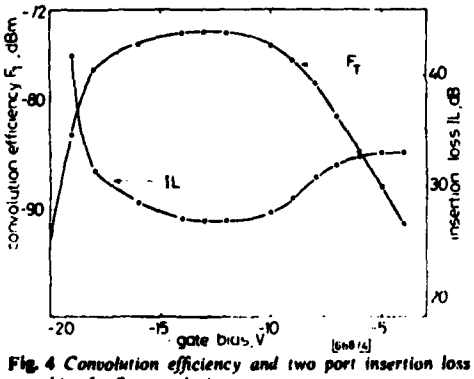

Fig. 4 *Convolution efficiency and two port insertion loss against DC gate bias for Sezawa device*

The fabricated Sezawa convolver had a synchronous frequency of $f_0 = 355$ MHz and a two port insertion loss of 27 dB. This synchronous frequency is 130 MHz higher than any previously reported MZOS Sezawa convolver.[7] A maximum convolver efficiency of $F_T = -74$ dBm was obtained and the convolution efficiency and insertion loss against gate bias are shown in Fig. 4.

In conclusion we have fabricated MZOS Rayleigh and Sezawa convolvers utilising separate comb grating transducers to obtain higher frequency devices than previously reported.[3,7] The Rayleigh device had a 285 MHz synchronous frequency and a maximum convolution efficiency of $F_T = -89$ dBm. The Sezawa device had a synchronous frequency of 355 MHz and a maximum convolution efficiency of $F_T = -74$ dBm.

This work was sponsored jointly by the US Air Force Office of Scientific Research under grant AFOSR-77-3304, the National Science Foundation under grant ECS-8103744, and the NSF-MRL grant DMR 77-23798.

M. R. MELLOCH
R. L. GUNSHOR
R. F. PIERRET

School of Electrical Engineering
Purdue University, West Lafayette, IN 47907, USA

17th August 1981

References

1 MELLOCH, M. R., GUNSHOR, R. L., and PIERRET, R. F.: 'Single phase and balanced separate comb transducer configurations in a ZnO/Si SAW structure', *IEEE Trans.*, to be published
2 YAO, I.: 'High performance elastic convolver with parabolic horns' Proc. IEEE ultrasonics symposium, 1980, pp. 37-42
3 ELLIOTT, J. K., GUNSHOR, R. L., PIERRET, R. F., and DAVIS, K. L.: 'Zinc oxide-silicon monolithic acoustic surface wave optical image scanner', *Appl. Phys. Lett.*, 1975, **27**, pp. 179-182
4 DAVIS, K. L.: 'Storage of optical patterns in a zinc-oxide-on-silicon surface wave convolver', *ibid.*, 1975, **26**, pp. 143-145
5 KINO, G. S., LUDVIK, S., SHAW, H. J., SHREVE, W. R., WHITE, J. M., and WINSLOW, D. K.: 'Signal processing by parametric interactions in delay-line devices', *IEEE Trans.*, 1973, **SU-20**, pp. 162-173
6 PIERRET, R. F., GUNSHOR, R. L., and CORNELL, M. E.: 'Charge injection in metal-ZnO-SiO_2-Si structures', *J. Appl. Phys.*, 1979, **50**, pp. 8112-8124
7 ELLIOTT, J. K., GUNSHOR, R. L., PIERRET, R. F., and DAY, A. R.: 'A wideband SAW convolver utilizing Sezawa waves in the metal-ZnO-SiO_2-Si configuration', *Appl. Phys. Lett.*, 1978, **32**, pp. 515-516

0013-5194/81/220827-02$1.50/0

LOW-LOSS MULTIFIBRE CONNECTORS WITH PLUG-GUIDE-GROOVED SILICON

Indexing terms: Optical fibres, Silicon

Low-loss interchangable multifibre connectors have been developed using plugs consisting of large guiding grooved and fibre-fixing V-grooved silicon chips. Guiding grooves etched on silicon chips accomplish extremely small average fibre offset less than 2 μm. A 6-fibre connector plug pair selected from the same wafer exhibits 0·14 dB average connection loss. Connector plugs from different wafers exhibit 0·17 dB and 0·24 dB average connection losses.

Introduction: Demountable and interchangable multifibre connectors are exceedingly useful in connecting cables and equipments. The connectors consist of a pair of plugs and mechanisms for plug alignment. The fibres must be located accurately in the plugs and each pair of plugs must be aligned accurately to attain low connecting loss. Many kinds of multifibre connectors have been reported up to this time. V-grooved connectors are suitable to connect ribbon fibres.

Miller[1] developed a multifibre splicer using precise V-grooved silicon chips. On the other hand, Fujii *et al.*[2]

Sezawa to Rayleigh mode conversion in the ZnO-on-Si surface acoustic wave device configuration

M. R. Melloch, R. L. Gunshor, and R. F. Pierret
School of Electrical Engineering, Purdue University, West Lafayette, Indiana 47907

(Received 3 June 1981; accepted for publication 19 June 1981)

Conversion of Sezawa surface waves to Rayleigh surface waves by means of an aluminum grating in the metal-ZnO-SiO_2-Si surface acoustic wave structure is reported. This conversion must be taken into account in the design of grating structures in ZnO-on-Si devices, such as multistrip couplers, to avoid unwanted stop bands. The conversion also provides a new phenomenological basis for the construction of bandpass filters.

PACS numbers: 43.35.Pt, 68.30. + z, 62.30. + d

The multistrip coupler[1] (MSC) represents an important component of many surface acoustic wave (SAW) devices.[2] The essence of the MSC is an ability to transfer SAW energy from one acoustic beam "track" to another. In order to construct multistrip couplers which are capable of implementing an energy transfer in some reasonable propagation length, a large electromechanical coupling coefficient k^2 is required. By exhibiting a substantial k^2, lithium niobate, for example, is a good candidate for MSC structures, while quartz (to cite another widely used SAW material) is not. A SAW configuration of current interest is the monolithic (MZOS) structure consisting of piezoelectric films of ZnO sputtered onto an oxidized silicon wafer. Although bulk ZnO is not characterized by strong piezoelectricity, it happens that a particular mode of the MZOS layered structure, the Sezawa mode, exhibits an electromechanical coupling comparable to $LiNbO_3$.[3] The implication is that the Sezawa mode propagating in the MZOS structure represents a good candidate for implementing the MSC concept. Initial experiments designed to employ such MSC structures have revealed a problem which we have attributed to a coupling of the Sezawa mode to the Rayleigh mode within the multistrip coupler. Shown in Fig. 1 is the measured transmission through an MSC structure revealing a deep stop band which we have identified as resulting from a conversion of energy initially in the Sezawa mode to the Rayleigh mode, as a result of the presence of the periodic MSC structure. A related phenomena has recently been observed in $LiNbO_3$ devices, wherein a surface acoustic wave was found to be converted into bulk plate modes as a result of the presence of a shallow-etched grating structure.[4,5]

The mechanism for the observed mode conversion can be explained by considering what occurs when a Sezawa surface wave of variation $\exp[i(k_s x - \omega t)]$ is incident on a grating of periodicity d. It can be shown that one expects modes having a variation given by $\exp\{i[(k_s + n2\pi/d)x - \omega t]\}$ are generated due to the perturbation of period d imposed by the MSC grating.[6] k_s is the wave number of the Sezawa wave and n is an integer. The phase velocity for a generated mode propagating in the x direction is given by

$$v_p = \omega/(k_s + n2\pi/d). \tag{1}$$

Setting $n = -1$, one obtains a specific phase velocity, and a corresponding wave number given by

$$k_R = k_s - 2\pi/d. \tag{2}$$

Clearly, when the grating periodicity d is less than the incident Sezawa wavelength λ_s, the $n = -1$ mode will propagate in a direction opposite to the incident Sezawa wave. Similarly if $d > \lambda_s$, then the $n = -1$ mode will propagate in the same direction as the incident Sezawa wave.

In order to experimentally verify the expected conversion of a Sezawa surface mode to the Rayleigh surface mode, the test device shown in Fig. 2 was used. The 7-Ω cm silicon wafer was of (100) orientation with propagation in the ⟨100⟩ direction. A 0.12-μm SiO_2 layer was thermally grown. The rf-sputtered ZnO film had a thickness of 6.5 μm. The test gratings consisted of either 300 or 400 aluminum strips with a periodicity of 15.24 μm. Transducers $S1$ and $S2$ consisted of ten finger pair interdigital transducers (IDT) of wavelength $\lambda_s = 40.64\,\mu$m. Transducer R was a 20 finger separate comb[7] interface[8] transducer of wavelength $\lambda_R = 24.4\,\mu$m. For the particular thickness, wave number product ($hk_R = 1.67$), an interface transducer was used to provide a much greater electromechanical coupling than is available

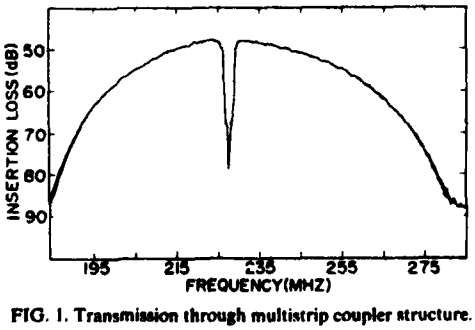

FIG. 1. Transmission through multistrip coupler structure.

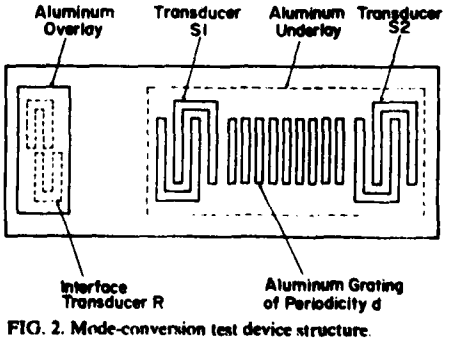

FIG. 2. Mode-conversion test device structure.

 0003-6951/81/180476-02$00.50

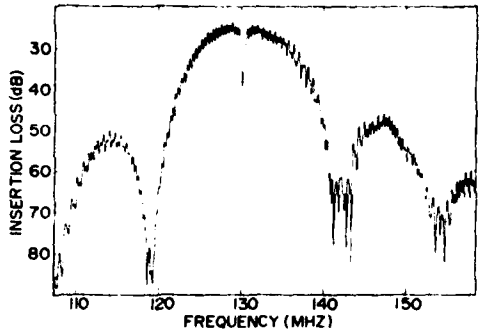

FIG. 3. Sezawa mode transmission through 400 strip Aluminum grating.

using more conventional construction where the IDT is located on the top of the ZnO film.

The transmission response from transducer $S1$ to transducer $S2$ is shown in Fig. 3. A narrow stop band of 15-dB depth was observed at a frequency of 130 MHz; the stop band was interpreted as corresponding to conversion from the Sezawa mode to the Rayleigh mode. Equations (1) and (2) can be used to obtain the phase velocity and propagation constant for the generated Rayleigh mode, yielding $v_p = 3.18\times10^5$ cm/sec and $k_R = 2\pi/24.4$ rad/cm, respectively. The value of 3.18×10^5 corresponds to the predictions of Rayleigh wave dispersion characteristics at $hk_R = 1.67$.

Because the test device grating periodicity is less than the wavelength of transducer $S1$, a Sezawa wave launched by transducer $S1$ will be converted by the grating into a Rayleigh mode which can be detected at transducer R. The top trace of the photograph in Fig. 4(a) shows the input pulse to transducer $S1$ at a frequency of 130 MHz. The first pulse appearing in the lower trace represents direct detection of the Sezawa wave by transducer R. The triangular-shaped response arises from the "backscattered" Rayleigh wave which was generated in the grating. The shape of the detected Rayleigh pulse is determined by the convolution of the Sezawa pulse with the grating array. With an acoustic absorber on the grating, the output obtained at transducer R is as shown in the photograph of Fig. 4(b). The response here consists of only the directly detected Sezawa mode. Since the bandwidths of the transducers were significantly greater than that of the grating, the mode conversion bandwidth is determined primarily by the length of the grating. A 3-dB bandwidth of 0.84 MHz was obtained for a grating of 300 strips.

In conclusion, we have demonstrated mode conversion between Sezawa and Rayleigh waves at a periodic grating in the MZOS device structure. The occurrence of such a conversion must be considered in the design of grating structures, such as the multistrip coupler, in layered monolithic configurations. The mode conversion could result in unwanted stop bands; alternatively such stop bands could be used to implement specific desired filter characteristics.

The authors are grateful to Gary MaGee and the Naval Avionics Center for making some of the photomasks used in device fabrication. This work was sponsored jointly by the Air Force Office of Scientific Research under Grant No. AFOSR-77-3304, the National Science Foundation under Grant No. ECS-8103744, and the NSF-MRL under Grant No. DMR 77-23798.

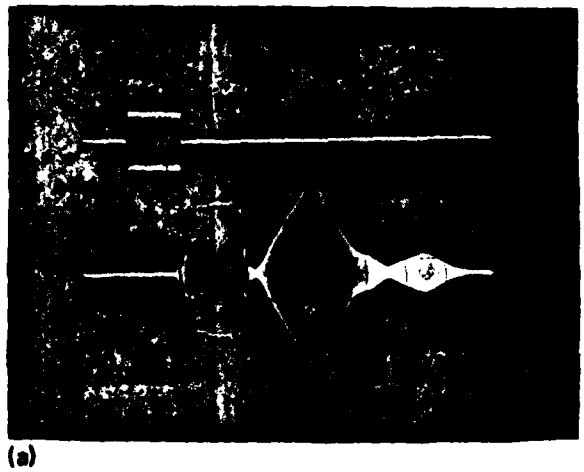

(a)

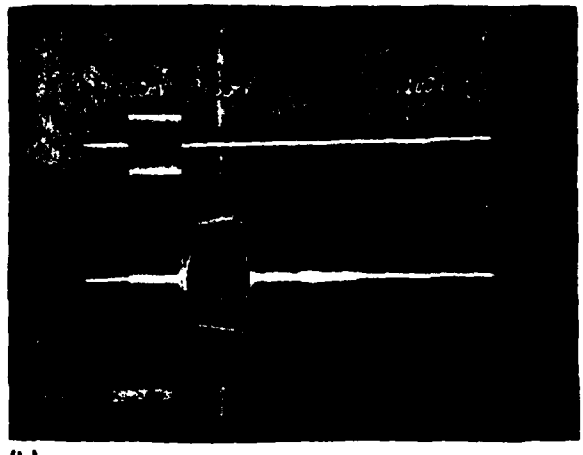

(b)

FIG. 4. (a) Oscillograph of input to transducer $S1$ and output on transducer R. (b) Oscillograph of input to transducer $S1$ and output on transducer R with an acoustic absorber on the aluminum grating.

[1]F. G. Marshall, C. O. Newton, and E. G. S. Paige, IEEE Trans. Sonics Ultrason. SU-20, 124 (1973).
[2]F. G. Marshall, C. O. Newton, and E. G. S. Paige, IEEE Trans. Sonics Ultrason. SU-20, 134 (1973).
[3]J. K. Elliott, R. L. Gunshor, R. F. Pierret, and A. R. Day, Appl. Phys. Lett. 32, 515 (1978).
[4]J. Melngailis, H. A. Haus, and A. Lattes, Appl. Phys. Lett. 35, 324 (1979).
[5]J. Melngailis and R. C. Williamson, in 1978 *Ultrasonics Symposium Proceedings*, IEEE Cat. No. 78CH1344-1SU (IEEE, New York, 1978).
[6]H. A. Haus, A. Lattes, and J. Melngailis, IEEE Trans. Sonics Ultrason. SU-27, 258 (1980).
[7]M. R. Melloch, R. L. Gunshor, and R. F. Pierret, "Single Phase and Balanced Separate Comb Transducer Configurations in a ZnO Saw Structure" (unpublished).
[8]M. R. Melloch, R. L. Gunshor, C. L. Liu, and R. F. Pierret, Appl. Phys. Lett. 37, 147 (1980).

APPENDIX D

CONVERSION OF SEZAWA TO RAYLEIGH WAVES IN THE ZnO-SiO_2-Si CONFIGURATION

M. R. Melloch, R. L. Gunshor, and R. F. Pierret

School of Electrical Engineering, Purdue University
West Lafayette, Indiana 47907

Abstract

The high electromechanical coupling of the Sezawa mode makes it feasible to construct devices such as a multistrip coupler in the metal-ZnO-SiO_2-Si surface acoustic wave configuration. The transmission of a 21.8 μm wavelength Sezawa surface wave through an 8.1 μm aluminum grating multistrip coupler, however, exhibited a narrow stopband. This stopband has been identified as resulting from a conversion of the Sezawa mode to the Rayleigh mode. Clearly, the mode conversion must be taken into account in the design of periodic grating structures, such as a multistrip coupler, to avoid spurious stopbands. The conversion also provides a new phenomenological basis for the construction of narrow bandpass filters.

I. Introduction

The multistrip coupler (MSC) [1] is an important conponent in many surface acoustic wave (SAW) device structures [2]. The essence of the MSC is an ability to transfer SAW energy from one acoustic track to another. One application of particular importance is the use of an MSC beam compressor in a $LiNbO_3$ SAW convolver configuration [3]. The compression of the acoustic wave by the MSC increases the power density in the SAW, which results in an increase in the nonlinear interaction, and hence an increase in the convolver efficiency [4]. It is important to note that the use of the MSC to compress the beam, rather than employing transducers with a narrow aperture, results in an increase in the dynamic range for the device [5].

We have investigated the possible use of the MSC as a component in the monolithic metal-ZnO-SiO_2-Si (MZOS) configuration. Since the length of transfer of SAW energy in an MSC is dependent on the electromechanical coupling, the first order Rayleigh mode is not a likely condidate for MSC structures. However, the Sezawa mode (second order Rayleigh mode) exhibits an electromechanical coupling comparable to $LiNbO_3$ [6], and hence is a promising candidate for MSC structures. Initial experiments to employ the MSC concept in the Sezawa MZOS configuration has led to the observation of an unanticipated phenomenon. Figure 1 shows the transmission through the MSC structure revealing a deep stopband. We have attributed this stopband to a conversion of the Sezawa mode to the Rayleigh mode, due to the presence of the periodic MSC structure. A similar phenomenon has recently been observed in $LiNbO_3$ devices, where a surface acoustic wave was converted to bulk plate modes due to the presence of a shallow etched grating structure [7,8].

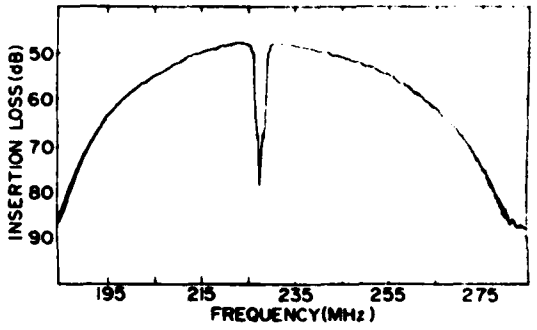

Fig. 1. Transmission through multistrip coupler structure.

In this paper we discuss the phenomenon of mode conversion due to periodic structures. Experimental support will then be presented for Sezawa to Rayleigh mode conversion in the MZOS configuration due to periodic perturbations in the SAW path. Conversion resulting from the presence of aluminum and shallow etched groove gratings will be demonstrated.

II. Discussion

The mechanism for mode conversion can be explained by considering what occurs when a Sezawa surface mode of variation $\exp[i(k_s x-\omega t)]$ is incident on a grating of periodicity d. The grating imposes periodic boundary conditions which are satisfied by the generation of space harmonics at frequency ω. The ω-k diagram in figure 2 can be used to demonstrate a conversion from one mode to another. Two modes are pictured, v_s and v_r, which are assumed dispersionless for the purposes of illustration. When the mode with wave number k_s is incident on the grating of periodicity d, the wave numbers are conserved if a spatial harmonic of wave number $k_r = k_s - \frac{2\pi}{d}$ at frequency ω is excited. Similarly if one shifts the ω-k curve for the r mode so it is centered at $n\frac{2\pi}{d}$, one obtains the following condition for the wave number of the generated mode at frequency ω.

$$k_m = k_s - n\frac{2\pi}{d} \qquad (1)$$

The phase velocity for the generated modes are given by,

0090-5607/81/0000-0765 $00.75 © 1981 IEEE

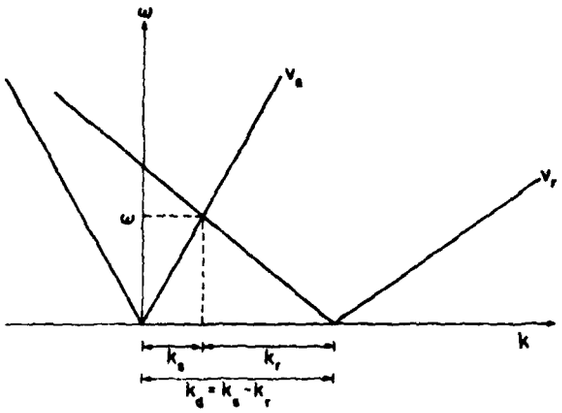

Fig. 2. ω-k diagram for two non-dispersive modes, v_s and v_r

$$v_{rn} = \frac{\omega}{k_s - n\frac{2\pi}{d}} \qquad (2)$$

If one sets n = 1 in equations (1) and (2), a specific phase velocity is obtained together with a corresponding wave number given by,

$$v_r = \frac{\omega}{k_s - \frac{2\pi}{d}} \qquad (3)$$

$$k_r = k_s - \frac{2\pi}{d} \qquad (4)$$

If the wavelength of the incident Sezawa mode, λ_s, is greater than the grating periodicity, d, then the generated Rayleigh mode will propagate in a direction opposite to the incident Sezawa mode. Similarly if $d > \lambda_s$, then the Rayleigh mode will propagate in the same direction as the incident Sezawa mode.

III. Experimental Results

A top view of the test device structure is illustrated in figure 3. The dashed lines represent metal patterns

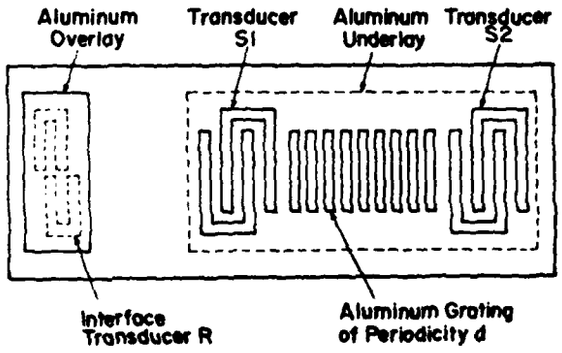

Fig. 3. Mode conversion test device structure.

positioned at the ZnO-SiO_2 interface, while the solid lines represent metal patterns located on top of the ZnO.

The test devices were fabricated on a 7 Ω-cm n-silicon wafer of (100) orientation with the SAW propagation in the silicon [100] direction. A 0.12 μm SiO_2 film was thermally grown, after which a 6.5 μm ZnO film was deposited by rf sputtering. The test gratings consisted of either 300 or 400 aluminum strips of periodicity d = 15.24 μm. Situated at both ends of the grating were interdigital transducers, S1 and S2, consisting of 10 aluminum finger pairs of wavelength λ_s = 40.65 μm. Beneath the grating and transducers S1 and S2 was an aluminum underlay at the ZnO-SiO_2 interface. Transducer R was a separate comb [9] interface [10] transducer, with 20 fingers in each parallel half of the transducer, designed for a wavelength of λ_r = 24.4 μm. Located above transducer R was a metal overlay on top of the ZnO. For the particular thickness-wave number product of $hk_r \approx 1.67$, the interface transducer was used to provide greater electromechanical coupling than is possible with the more conventional construction where the transducer is located on top of the ZnO [11]. For the relatively short wavelength of λ_r = 24.4 μm, a separate comb transducer was chosen to improve device yields.

The transmission response from transducer S1 to S2 is shown in figure 4 for a device with a 400 aluminum strip grating. A 15 dB deep stopband, which has been

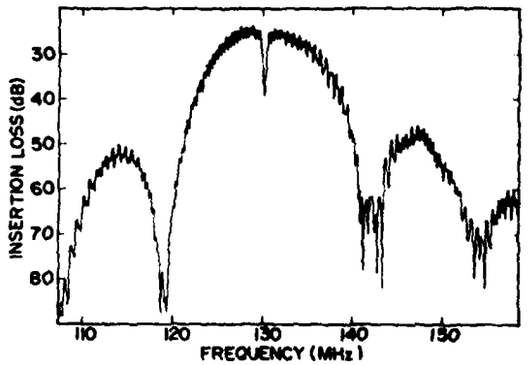

Fig. 4. Sezawa mode transmission through 400 strip aluminum grating.

attributed to conversion from the Sezawa to Rayleigh mode, was observed at a frequency of 130 MHz. The phase velocity and wave number for the generated Rayleigh mode can be obtained from equations (3) and (4). The resulting phase velocity, $v_r = 3.18 \times 10^5 \frac{cm}{sec}$, and the thickness-wave number product, $hk_r = \frac{2\pi}{24.4}\frac{rad}{cm} = 1.87\frac{rad}{cm}$, are found to correspond to computed Rayleigh wave dispersion characteristics [12]. For test devices having gratings formed from 300 aluminum strips, stopbands of approximately 10 dB depth were obtained.

Pulse measurement techniques have been used to further investigate the Sezawa to Rayleigh mode conversion. Transducer S1 is constructed with a wavelength, λ_s, which is larger than the grating periodicity, d. A Sezawa wave launched by this transducer will be converted by the grating to a Rayleigh mode, which can be

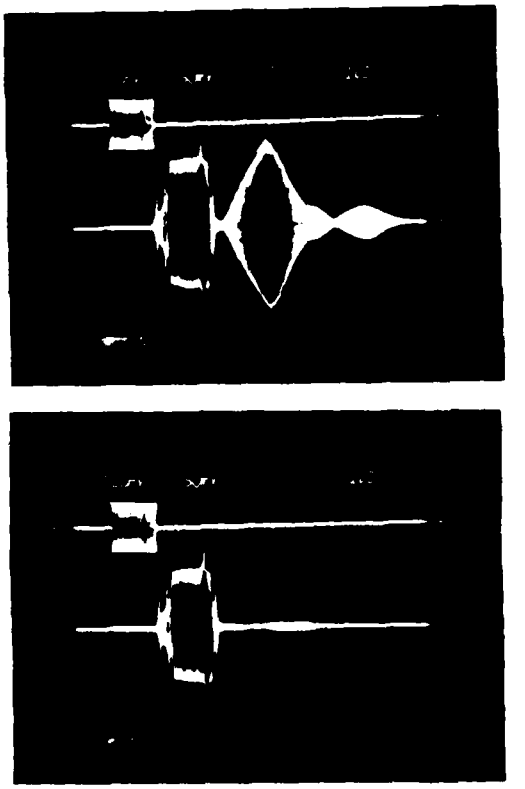

Fig. 5.(a)Oscillograph of input to transducer S1 and output of transducer R. (b)Oscillograph of input to transducer S1 and output of transducer R with an acoustic absorber on the aluminum grating.

detected by transducer R. The top trace in figure 5a shows the input pulse to transducer S1. The first pulse in the bottom trace of figure 5a represents the direct detection of the Sezawa pulse launched on transducer S1. The first larger triangular shaped pulse is due to the Rayleigh mode generated in the grating. The shape of this detected Rayleigh pulse is determined by the convolution of the incident Sezawa pulse and the test grating. The second smaller triangular shaped pulse is due to the Sezawa to Rayleigh conversion of the reflected Sezawa wave obtained as the result of direct detection at transducer R. With an acoustic absorber on the test grating, the output of transducer R consists only of the directly detected Sezawa pulse, as shown in figure 5b. Since the bandwidths of the transducers are significantly greater than that of the grating, the mode conversion bandwidth is determined by the length of the grating. Figure 6 displays the frequency response of the mode conversion from transducer S1 to transducer R for a 300 aluminum strip grating. A 3 dB bandwidth of 0.84 MHz was obtained.

Since efficient conversion of surface acoustic waves to bulk plate modes, due to shallow etched grooves, has been observed in $LiNbO_3$ [7,8], shallow grooves were examined in a second MZOS test device. Here the aluminum grating pattern was used as a mask for etching the ZnO, and subsequently the aluminum grating was removed.

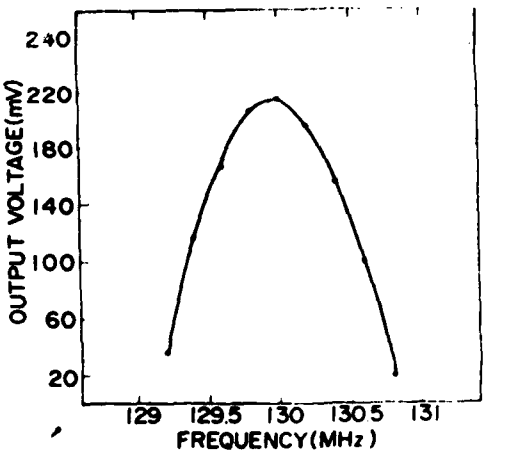

Fig. 6. Frequency response of mode conversion from transducer S1 to transducer R for a 300 aluminum strip grating.

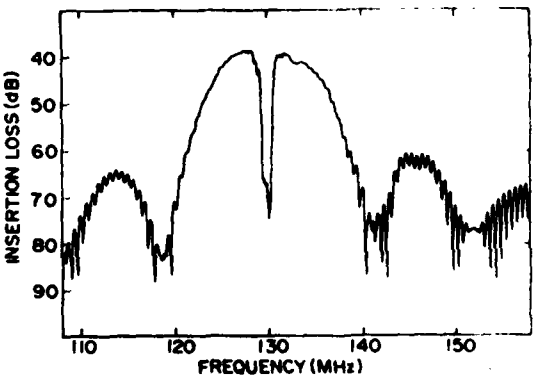

Fig. 7. Sezawa mode transmission through 300 groove 0.2 μm deep grating.

The mode conversion for a 300 groove 0.2 μm deep grating is shown in figure 7. A 35 dB deep stopband was obtained for this device compared to the 10 dB deep stopband observed with the 300 strip aluminum grating structure.

The conversion for another 300 groove grating, which has 0.1 μm deep grooves, is shown in figure 8. The stopband for this device was approximately 19 dB deep. It appears the perturbations imposed by the grooved gratings are much more efficient for mode conversion than are the aluminum grating structures.

IV. Conclusion

The conversion between the Sezawa and the Rayleigh mode, due to both periodic aluminum strip arrays and etched grooved arrays, has been demonstrated in the MZOS monolithic device configuration. In order to avoid unwanted stopbands, the occurrence of such a conversion must be considered in the design of grating structures, such as the multistrip coupler, in layered

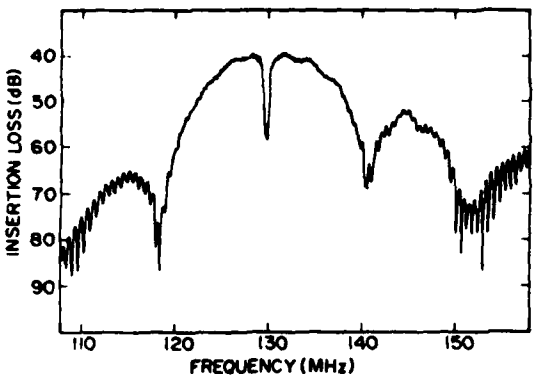

Fig. 8. Sezawa mode transmission through 300 groove 0.1 μm deep grating.

monolithic configurations. Alternatively, such stopbands could be used to implement desired filter characteristics.

V. Acknowledgements

The authors are grateful to Gary MaGee, Steve Phillips, and the Naval Avionics Center for making some of the photomasks used in device fabrication.

This work was sponsored jointly by the Air Force Office of Scientific Research under Grant No. AFOSR-77-3304, The National Science Foundation under Grant No. ECS-8103744, and the NSF-MRL Grant DMR 77-23798.

References

[1] F. C. Marshall, C. O. Newton, and E. G. S. Paige, "Theory and Design of the Surface Acoustic Wave Multistrip Coupler", *IEEE Trans. Sonics Ultrason.*, vol. SU-20, pp. 124-133, April 1973.

[2] F. C. Marshall, C. O. Newton, and E. G. S. Paige, "Surface Acoustic Wave Multistrip Components and Their Applications", *IEEE Trans. Sonics Ultrason.*, vol. SU-20, pp. 134-143, April 1973.

[3] P. Defranould and C. Maerfeld, "Acoustic Convolver Using Multistrip Beamwidth Compressors", *Electron. Lett.*, vol. 10, pp. 209-210, May 1974.

[4] T. C. Lim, E. A. Kraut, and R. B. Thompson, "Nonlinear Materials for Acoustic-Surface-Wave Convolver", *Appl. Phys. Lett.*, vol. 20, pp. 127-129, February 1972.

[5] Philippe Defranould and Charles Maerfeld, "A SAW Planar Piezoelectric Convolver", *Proceedings of the IEEE*, vol. 64, pp. 748-751, May 1976.

[6] J. K. Elliott, R. L. Gunshor, R. F. Pierret, and A. R. Day, "A Wideband SAW Convolver Utilizing Sezawa Waves in the metal-ZnO-SiO_2-Si Configuration", *Appl. Phys. Lett.*, vol. 32, pp. 515-516, May 1978.

[7] J. Melngailis and R. C. Williamson, "Interaction of Surface Waves and Bulk Waves in Gratings: Phase Shifts and Sharp Surface-Wave/Reflected Bulk Wave Resonances", 1978 Ultrasonics Symposium Proceedings, pp. 623-629.

[8] J. Melngailis, H. A. Haus, and A. Lattes, "Efficient Conversion of Surface Acoustic Waves in Shallow Gratings to Bulk Plate Modes", *Appl. Phys. Lett.*, vol. 35, pp. 324-326, August 1979.

[9] M. R. Melloch, R. L. Gunshor, and R. F. Pierret, "Single Phase and Balanced Separate Comb Transducer Configurations in a ZnO SAW Structure", *IEEE Trans. Sonics Ultrason.*, to be published.

[10] M. R. Melloch, R. L. Gunshor, C. L. Liu, and R. F. Pierret, "Interface Transduction in the ZnO-SiO_2-Si Surface Acoustic Wave Device Configuration", *Appl. Phys. Lett.*, vol. 37, pp. 147-150, July 1980.

[11] J. K. Elliott, R. L. Gunshor, and R. F. Pierret, "Zinc Oxide on Silicon Surface Acoustic Wave Devices for Signal Processing and Frequency Control", *Purdue University Technical Report*, TR-EE 78-33, July 1978.

[12] Phase velocity calculations were made utilizing a computer program written by K. L. Davis of the Naval Research Laboratory.

Aluminum nitride on silicon surface acoustic wave devices

L. G. Pearce, R. L. Gunshor, and R. F. Pierret
School of Electrical Engineering, Purdue University, West Lafayette, Indiana 47907

(Received 3 August 1981; accepted for publication 9 September 1981)

Reactive rf planar magnetron sputtering has been used at substrate temperatures below 300 °C to deposit highly oriented piezoelectric AlN films on silicon for surface acoustic wave device applications. The substrates were (100)-oriented, *n*-type silicon with and without a thermally grown oxide. Several new AlM-on-silicon surface acoustic wave devices were fabricated and tested. The devices reported herein include two-port delay lines, degenerate monolithic convolvers, and two-port surface acoustic wave resonators utilizing metal strip reflector arrays.

PACS numbers: 43.35.Pt, 43.88.Fx, 85.90. + h

One branch of the development of surface acoustic wave (SAW) devices emphasizes the integration of SAW with semiconductors. Specifically, there has been a considerable effort to launch and propagate surface acoustic waves on silicon by employing thin sputtered films on ZnO on oxidized silicon substrates. Aluminum nitride is another material which has been considered for use as a piezoelectric thin film for SAW applications. The properties of chemical stability, mechanical strength, high acoustic velocity, and good dielectric qualities make AlN an attractive alternative ZnO for monolithic SAW devices.[1]

The formation of piezoelectric AlN films for SAW studies has until recently been achieved only by using substrate temperatures in excess of 1000 °C. Although chemical vapor deposition methods will always require such high temperatures,[2] successful deposition of piezoelectric films at much lower temperatures onto glass and sapphire substrates has lately been accomplished by reactive sputtering.[3] Processing at these lower temperatures is more compatible with existing silicon technology and enhances the appeal of an integrated AlN-silicon structure. We report here on the performance of some new AlN-on-silicon SAW devices (Fig. 1) fabricated by reactive rf planar magnetron sputtering with substrate temperature below 300 °C.

The system used to deposit the AlN films was an MRC 8620 Sputtering Head with a magnetron cathode assembly. A 99.999% aluminum target was situated 3.6 cm above the heated substrate platform. During the sputtering a total chamber pressure of approximately 8 mT was maintained with a gas mixture of 60% nitrogen and 40% argon. The depositions were performed with between 250 and 300 W of rf input power resulting in a sputtering potential of about 130 V and a substrate platform temperature of 260 °C. Under these conditions a deposition rate of approximately 0.3 μm per hour was achieved.

Films having a thickness of approximately 1.5 μm were deposited on (100)-oriented, *n*-type silicon substrates having a resistivity of about 10 Ω cm. Appearing smooth and clear, the films produced strong x-ray diffractometer response peaks at $2\theta = 36.2°$. This peak corresponds to AlN oriented with the *c* axis normal to the silicon substrate surface.

The AlN monolithic structure has been examined in several device configurations. Figure 2 shows the frequency response of an AlN/SiO_2/Si delay line. The thermally grown oxide layer on the silicon was 0.12 μm thick, and the AlN film thickness was 1.6 μm. Interdigital transducers (IDT's) with ten finger pairs were formed by etching a 1000 Å evaporated aluminum layer. The transducers were driven balanced with respect to the substrate in order to surpress elec-

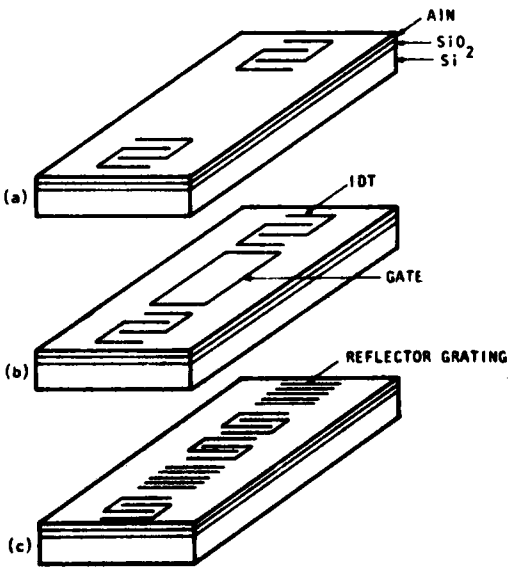

FIG. 1. (a) Two-port delay line; (b) degenerate convolver; (c) two-port resonator.

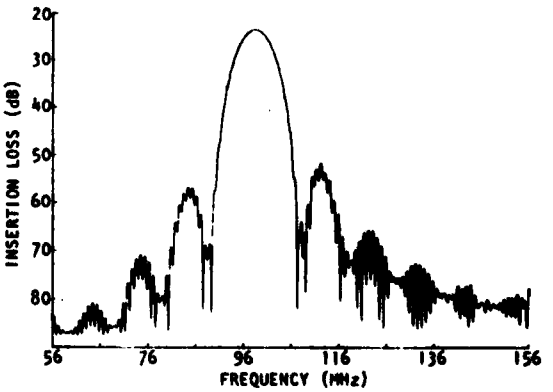

FIG. 2. Delay line frequency response for AlN/SiO_2/Si device.

 0003-6951/81/230878-02$00.50

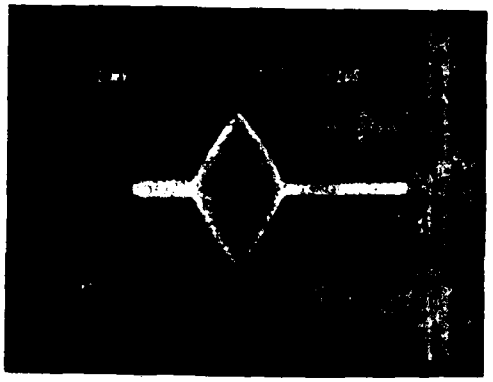

FIG. 3. High-pass filtered and 30 dB amplified convolution output for pulse envelope imputs of 3-μs length.

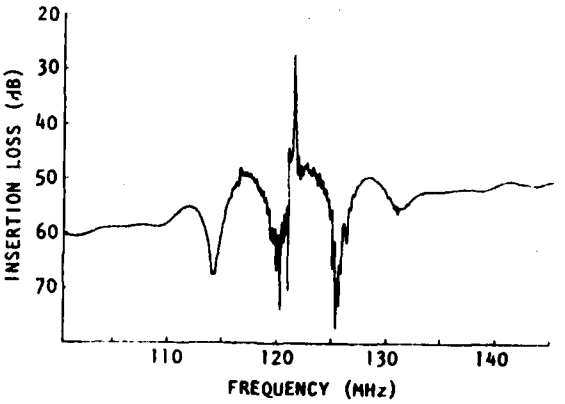

FIG. 4. Frequency response for two-port resonator with reflectors of 400 shorted gold strips.

tromagnetic direct coupling, and tuning was accomplished with series inductors. At the center frequency of 98.05 MHz, an insertion loss of 23.5 dB was measured along with a fractional bandwidth of 6.3%. The propagation path between transducer centers was 5.6 mm, the wavelength was 50.8 μm, and the time delay was 1.1 μs.

The same AlN/SiO_2/Si medium as described above was used in the fabrication of a degenerate acoustoelectric convolver. Ten-finger pair aluminum IDT's with a 35.6-μm period were placed at either end of a 1.4-cm-long aluminum gate electrode. A tuned delay line insertion loss of 34.7 dB was obtained at a center frequency of 141.7 MHz. Although some charge injection was evident in capacitance-voltage (C-V) measurements, the optimum gate bias for convolution was constant after the first few minutes of operation at a bias value of -14.7 V. The convolution output for equal-pulse envelope inputs is shown in Fig. 3. Input signals were 20 dBm each and yielded a bilinear convolution efficiency of -101.4 dBm.

Another convolver was constructed on a substrate without the SiO_2 layer and with 1.5 μm of AlN. In this case, twenty-finger pair transducers with the same periodicity as above were utilized. At the center frequency of 141.0 MHz the delay line insertion loss was 28.6 dB, and the bilinear conversion efficiency was -96 dBm. The gate bias required for depletion of the silicon was markedly different in this case. A gate potential of $+22$ V was found to maximize the convolution output. Again, charge injection was evidenced in the C-V measurements, and the gate bias stabilized in a few minutes.

The third type of device examined in the AlN/SiO_2/Si structure was a two-port SAW resonator with gold transducers and reflector gratings. The transducers were comprised of eight-finger pairs each at a wavelength of 40.6 μm, and the reflector arrays consisted of 400 shorted gold strips. The frequency response for one such device is displayed in Fig. 4. In this particular case, the AlN was 1.6 μm thick and the gold thickness was 550 Å. The untuned response reveals a 27.3-dB insertion loss at a resonant frequency of 121.74 MHz with a loaded Q of 3370. (The wide lobes in the response at 50 dB are due to interference between the acoustic signal and electromagnetic direct coupling between the cavity transducers.) A third transducer was situated outside the cavity to allow transmission measurements through one of the gratings. The grating stop band depth for this device was measured to be 21.5 dB. Based on an impedance mismatch model,[4] this leads to a per strip reflectivity of 0.79%. Another device, with 630 Å of gold, exhibited a Q of almost 5000 but also admitted a second resonance peak, indicating that the cavity length was not optimized.

The results reported herein prove the feasibility of using low-temperature-sputtered AlN as a piezoelectric thin film on silicon. The device characteristics presented compare reasonably well with analogous ZnO devices.[5,6] These performances, however, do not represent optimized AlN-on-silicon devices. More information on the coupling and propagation losses of AlN-on-silicon will be needed before the full potential of this structure can be evaluated.

The authors wish to thank Dr. David Garrod for his discussions and assistance in this project. The authors are also grateful to Dr. C. R. Aita of Gould Laboratories, who, as a participant in a joint NSF university-industry research project (Grant No. ECS-8103744), contributed generously of her time to aid in the development of the techniques for AlN deposition. This work was also supported jointly by the Air Force Office of Scientific Research Grand AFOSR-77-3304 and the NSF-MRL Program DMR77 23798.

[1] J. H. Collins, P. J. Hagon, and G. R. Pulliam, Ultrasonics 8, 218 (1970).
[2] K. Tsubouchi, K. Sugai, and N. Mikoshiba, in 1980 *Ultrasonics Symposium Proceedings*, IEEE Cat. No. 80CH160-2 (IEEE, New York, 1980).
[3] T. Shiosaki, T. Yamamota, T. Ode, K. Harada, and A. Kawabata, in 1980 *Ultrasonics Symposium Proceedings*, IEEE Cat. No. 80CH1602-2 (IEEE, New York, 1980).
[4] P. S. Cross, IEEE Trans. Sonics Ultrason. 23, 255 (1976).
[5] G. S. Kino, in 1979 *Ultrasonics Symposium Proceedings*, IEEE Cat. No. 79CH1482-9 (IEEE, New York, 1979).
[6] S. J. Martin, R. L. Gunshor, and R. F. Pierret, Appl. Phys. Lett. 37, 200 (1980).

SPUTTERED ALUMINUM NITRIDE ON SILICON FOR SAW DEVICE APPLICATIONS

L. G. Pearce, R. L. Gunshor, and R. F. Pierret

School of Electrical Engineering, Purdue University
West Lafayette, Indiana 47907

Abstract

Reactive rf planar magnetron sputtering is employed to deposit piezoelectric aluminum nitride films on silicon substrates where the substrate temperature during deposition is below 300°C. The films, grown on substrates of both (100) and (111) oreinted silicon with and without the presence of a thermally grown oxide, are oriented with the c-axis normal to the substrate surface. We report the operating characteristics of several new AlN-on-silicon devices. These include two-port delay lines , degenerate monolithic convolvers, and surface acoustic wave resonators utilizing metal strip reflector arrays. The reported data includes electrical characteristics of the metal-AlN-(SiO_2)-Si sandwich, and dispersion properties for (100)-cut, <100>-propagating and (111)-cut, <211>-propagating substrates.

I. Introduction

The development of surface acoustic wave (SAW) technology has included significant efforts to integrate SAW with semiconductors. On silicon the most common approach has been to make use of a thin piezoelectric film of zinc oxide deposited by sputtering. Another material which has been considered for the role of the thin piezoelectric film is aluminum nitride. Chemical stability, mechanical strength, high acoustic velocity, and good dielectric qualities make AlN an attractive prospect for monolithic SAW devices on silicon [1].

Until recently the formation of piezoelectric AlN films for SAW application has been achieved only by methods employing substrate temperatures in excess of 1000°C. Although chemical vapor deposition methods will always require these high temperatures [2], successful deposition of piezoelectric AlN films at much lower temperatures has lately been accomplished by reactive sputtering onto glass and sapphire substrates [3]. This lower temperature processing is more compatible with silicon technology and enhances the appeal of the AlN-silicon structure. We report here on the performance of SAW devices (figure 1) constructed on this new layered structure fabricated by reactive rf planar magnetron sputtering with substrate temperatures below 300°C.

II. Experimental Results

The system used to deposit the AlN films was an MRC 8620 sputtering head fitted with a magnetron cathode assembly. An aluminum target of 99.999% purity was located 3.6 cm above the heated substrate platform. A chamber pressure of approximately 6mT was maintained

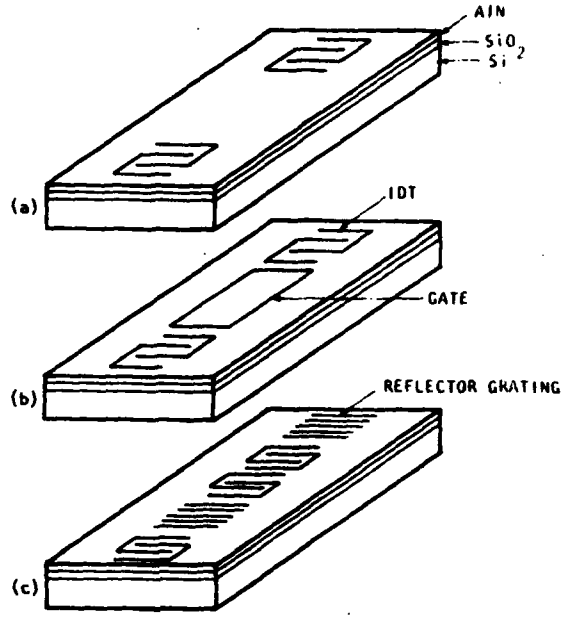

Fig. 1. AlN-on-Si device types; (a) delay line, (b) degenerate acoustoelectric convolver, (c) two port resonator.

with a gas mixture of 60% nitrogen and the remainder argon. Input rf power was between 250 and 300 watts and resulted in a sputtering potential of about 130 volts. The substrate platform was heated to a temperature of 280°C. With these conditions a deposition rate of approximately 0.3 μm per hour was obtained.

Films of approximately 1.5 μm thickness were deposited on substrates of n-type silicon with resistivity of about 10 Ω cm and of both (100) and (111) orientations. Substrates both with and without 1200Å of thermally grown oxide were used as well as substrates with 0.1 μm of evaporated aluminum covering the oxide. The films on all substrates appeared smooth and clear and produced strong x-ray diffractometer peaks at $2\theta=36.2°$. This diffraction response corresponds to AlN oriented with the c-axis normal to the substrate surface. The films exhibited a resistivity in excess of 10^{10} Ω-cm and a relative permittivity of 11.1.

0090-5607/81/0000-0381 $00.75 © 1981 IEEE

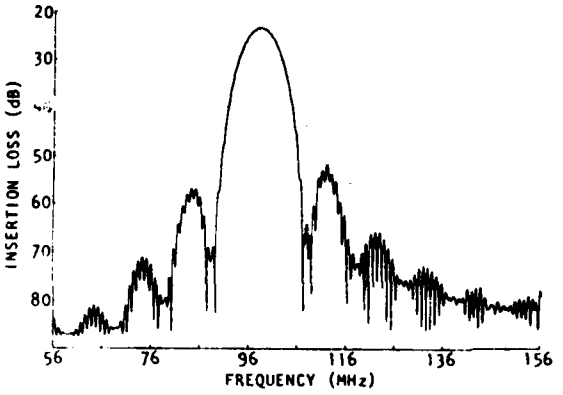

Fig. 2. Frequency response for AlN/SiO_2/Si (100)-cut, <100>-propagating delay line with λ= 50.8 μm and h = 1.6 μm.

Figure 2 shows the frequency response of a delay line on the AlN/SiO_2/Si(100) structure. For this device the AlN was 1.6 μm thick, and the acoustic wavelength was 50.8 μm. Interdigital transducers (IDT's) with ten finger pairs were etched from a 0.1 μm evaporated aluminum layer. Tuning was achieved with series inductors, and the transducers were driven balanced in order to minimize electromagnetic direct coupling. An insertion loss of 23.5 dB was measured at the center frequency of 98.05 MHz while the 5.6 mm path (between transducer centers) yielded a delay of 1.1 μsec.

Phase velocity data as a function of hk (film thickness times wave number) is plotted in figure 3. The phase velocity was found by taking the product of the wavelength and the delay line center frequency. Data here is for the AlN/Al/SiO_2/Si configuration of both silicon orientations. The phase velocities found are seen to fall very near the appropriate silicon Rayleigh wave velocities. This data indicates that, in the range examined, the AlN-silicon system behaves as a relatively low dispersion medium. This is of significant importance for applications where distortion due to dispersion must be minimized. For comparison the dispersion curves for the ZnO-silicon system are also shown. Attempts to measure the electromechanical coupling on these devies only succeeded in bounding the value of k^2 to between 0.10% and 0.16%, for the hk range examined.

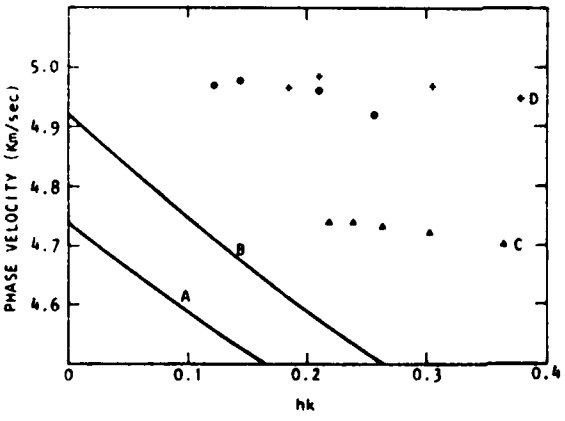

Fig. 3. Phase velocity vs. hk. Curves are the dispersion relation for ZnO-on-Si; data points are for the AlN/Al/SiO_2/Si devices. A and C are for (111)-cut, <211>-propagating substrates; B and D are for (100)-cut, <100>-propagating.

Two-port SAW resonators with gold metalization were constructed on the AlN/SiO_2/Si(100) structure. The reflector arrays consisted of 400 shorted gold strips of one quarter wavelength width and spacing, and the transducers were IDT's with eight finger pairs. Figure 4 displays the frequency response of one of these resonators. For this device the AlN was 1.6 μm, the gold 550Å

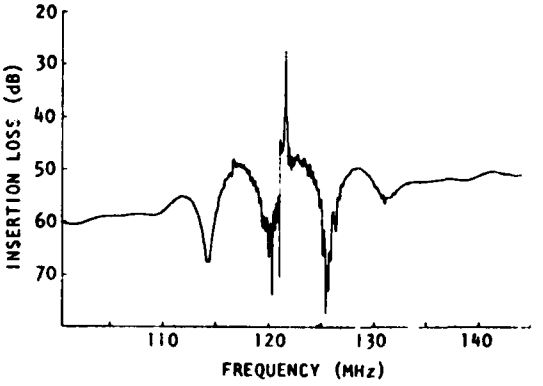

Fig. 4. Response for resonator on AlN/SiO_2/Si (100)-cut, <100>-propagating structure. Reflectors are 400 shorted gold strips, λ= 40.6 μm, h = 1.6 μm, and Q = 3370.

thick, and the wavelength was 40.6 μm. At the resonant frequency of 121.74 MHz an unloaded insertion loss of 7.3 dB was obtained, and a loaded Q of 3370 was measured. (The wide lobes in the response are due to interference between the acoustic signal and the electromagnetic direct coupling.) Transmission measurements through one of the reflection gratings were made using a third transducer placed outside the resonator cavity. The impedance mismatch model for gratings [4] associates a per strip reflectivity of 0.79% with the 21.5 dB stop band depth found. Other devices with thicker gold exhibited Q's up to 5000, but the cavity length was not optimized and allowed a second resonance peak.

A degenerate acoustoelectric convolver was fabricated on the AlN/SiO_2/Si(100) material. Aluminum IDT's with ten finger pairs and a periodicity of 35.6 μm were situated on both ends of a 1.4 cm long aluminum gate electrode. When operated as a delay line the device yielded a tuned insertion loss of 34.7 dB with a center frequency of 141.7 MHz. Hysteresis in the capacitance-voltage (C-V) measurements on the gate electrode indicate charge injection, but the gate bias to optimize the convolution output stabilized at a value of -14.7 volts. With input signals of +20 dBm each, a bilinear convolution efficiency of -101.4 dBm was obtained.

Another convolver was constructed on the layered structure without the SiO_2 region. Twenty finger pair

IDT's of 35.6 μm periodicity were used on the 1.5 μm thick AlN film. At the center frequency of 141.0 MHz a tuned insertion loss of 28.6 dB through the delay line was recorded. A bilinear convolution efficiency of -96 dBm was achieved at an optimum gate bias of plus 22 volts. Charge injection and bias stabilization were again observed.

III. Conclusions

The results reported herein demonstrate the feasibility of using low temperature sputtered AlN as a piezoelectric thin film on silicon. Characteristics for devices described here compare relatively well with analogous ZnO devices [5,6]. However, these devices do not represent optimized designs on the AlN-on-silicon structure. A full evaluation of the potential of this new layered medium for SAW will necessitate more information on the coupling, dispersion, and propagation loss.

IV. Acknowledgements

The authors wish to thank Dr. David Garrod for his discussions and assistance in this project. The authors are also grateful to Dr. C. R. Aita of Gould Laboratories, who, as a participant in an NSF joint university-industry research project (ECS-8009793), contributed generously of her time to aid in the development of the techniques for AlN deposition.

This work was also supported by the Air Force Office of Scientific Research Grant AFOSR-77-3304 and the NSF-MRL Program DMR 77 23798.

References

[1] J. H. Collins, P. J. Hagon, and C. R. Pulliam, "Evaluation of New Single Crystal Piezoelectric Materials for Surface-Wave Applications," *Ultrasonics*, vol. 8, pp. 218-226, October 1970.

[2] K. Tsubouchi, K. Sugai, and N. Mikoshiba, "High-Frequency and Low-Dispersion SAW Devices on AlN/Al_2O_3 and AlN/Si for Signal Processing," 1980 *Ultrasonics Symposium Proceedings*, pp. 446-450.

[3] T. Shiosaki, T.Yamamota, T. Ode, K. Harada, and A. Kawabata, "Low Temperature Growth of Piezoelectric AlN Film for Surface and Bulk Wave Transducers by RF Reactive Planar Magnetron Sputtering," 1980 *Ultrasonics Symposium Proceedings*, pp. 451-545.

[4] P. S. Cross, "Properties of Reflective Arrays for Surface Acoustic Resonators," *IEEE Trans. Sonics and Ultrasonics*, vol. SU-23, pp. 255-262, July 1976.

[5] G. S. Kino, "Zinc Oxide on Silicon Acoustoelectric Devices," 1979 *Ultrasonics Symposium Proceedings*, pp. 900-910.

[6] S. J. Martin, R. L. Gunshor, and R. F. Pierret, "Zinc-Oxide-on-Silicon Surface Acoustic Wave Resonators," *Appl. Phys. Lett.*, vol. 37, pp. 700-701, 15 October 1980.

BIAS STABLE ZINC OXIDE-ON-SILICON SURFACE ACOUSTIC WAVE DEVICES

R. D. Cherne, M. R. Melloch, R. L. Gunshor and R. F. Pierret

School of Electrical Engineering, Purdue University
West Lafayette, Indiana 47907

Abstract

Charge injection and trapping within the metal-ZnO-SiO_2-Si (MZOS) structure is the well-known cause of a serious bias instability routinely exhibited by ZnO-on-Si surface acoustic wave devices. Herein we report and describe the attainment of d.c. stable MZOS device structures. Through a simple modification in the standard MZOS fabrication procedure, devices have been produced which, under dark conditions, attain a repeatable d.c. operating point within seconds after applying the desired d.c. bias. Fabrication details, data illustrating the achieved degree of bias stability, and comparative surface acoustic wave device characteristics are presented. A physical model explaining the observed stability is also discussed.

Introduction

Charge injection and trapping within the metal-ZnO-SiO_2-Si (MZOS) structure is the well-known cause of the serious bias instability routinely exhibited by ZnO-on-Si Surface Acoustic Wave (SAW) devices [1-4]. Upon application of a negative bias to the gate, electrons are injected into the ZnO layer and become localized in deep level traps at or near the ZnO-SiO_2 interface [3]. Thermal emission from the traps under subsequent positive increments in gate voltage is quite slow, resulting in device characteristics that can be shifted by tens of volts (see Fig. 1) and which totally relax only after several days. The relaxation process can be accelerated by illuminating the structure, or pn junctions can be fabricated in the Si to partially circumvent the problem in certain device configurations [5]. Clearly, however, it would be desirable if the basic structure was capable of responding quickly to changes in the d.c. gate bias under normal operating conditions. Herein we report the successful fabrication of a truly bias stable ZnO-on-Si SAW device. As will be detailed, stability is achieved through the use of a simple low temperature anneal.

Experimental Results

To demonstrate both the achieved degree of bias stability and the fact that stability is not obtained at the expense of a degradation in SAW performance, test devices were fabricated and patterned as shown in Fig. 2. Pictured is a standard convolver (less the usual transducer underlays) and two adjacent capacitors included to facilitate probe measurements of the MZOS capacitance-voltage characteristics. The transducers,

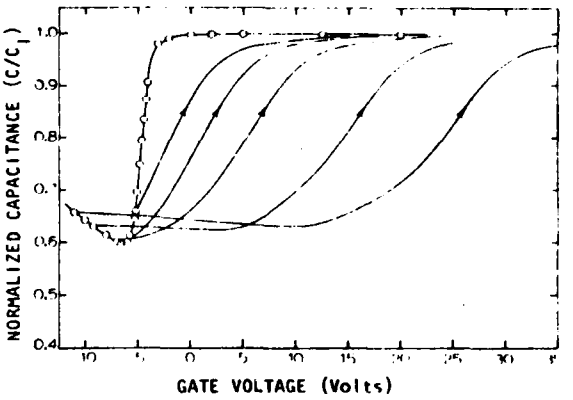

Fig.1. Sample set of stationary state (dots) and sweep-back characteristics typifying the charge injection/trapping phenomenon occurring in MZOS structures. (This figure is the same as Fig. 3 in reference 3.)

separated by a center-to-center spacing of 12.7 mm, contain twenty finger pairs with equal widths and gaps of 8.9 μm. The convolver beamwidth is 1.0 mm; the gate length is 10.2 mm. The adjacent MZOS capacitors have gate areas of 0.0324 cm^2. All devices were fabricated on 6-8 ohm-cm (100) oriented n-type Si wafers which were thermally oxidized to an SiO_2 thickness of 1000 Å. ZnO films, 1.9 μm thick, were deposited at a rate of 1.5 μm/hr using an rf magnetron sputtering system with a 99.999% pure ZnO target. The substrate platform was maintained at temperatures between 120 °C and 160 °C during all depositions. Following the growth of the ZnO layers, but prior to gate metallization, the structures were annealed for 60 min in a nitrogen atmosphere at temperatures ranging from 380 °C to 490 °C. It is the addition of this low temperature post-deposition anneal which results in the improved bias stability. The devices were completed by evaporating and patterning the aluminum metallization such that Rayleigh wave propagation occurred in a <100> direction.

Figures 3a and 3b respectively display the measured two-port insertion loss versus frequency and the bilinear conversion factor (F_T) versus gate bias (V_G) obtained from an N_2 annealed convolver. The pictured minimum insertion loss of 24 dB and maximum F_T of -72 dBm are quite typical for a Rayleigh wave convolver [6-8]. What is unusual, however, is attainment of a stable operating

0090-5607/81/0000-0780 $00.75 © 1981 IEEE

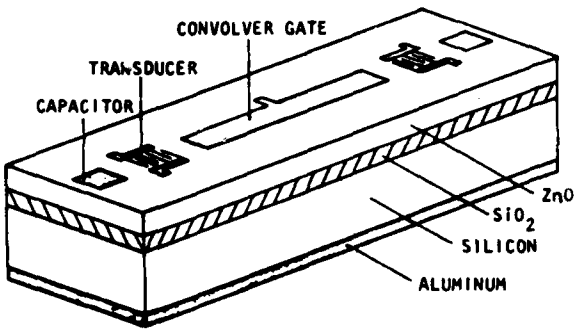

Fig.2.Experimental test structure consisting of two MZOS capacitors and a convolver.

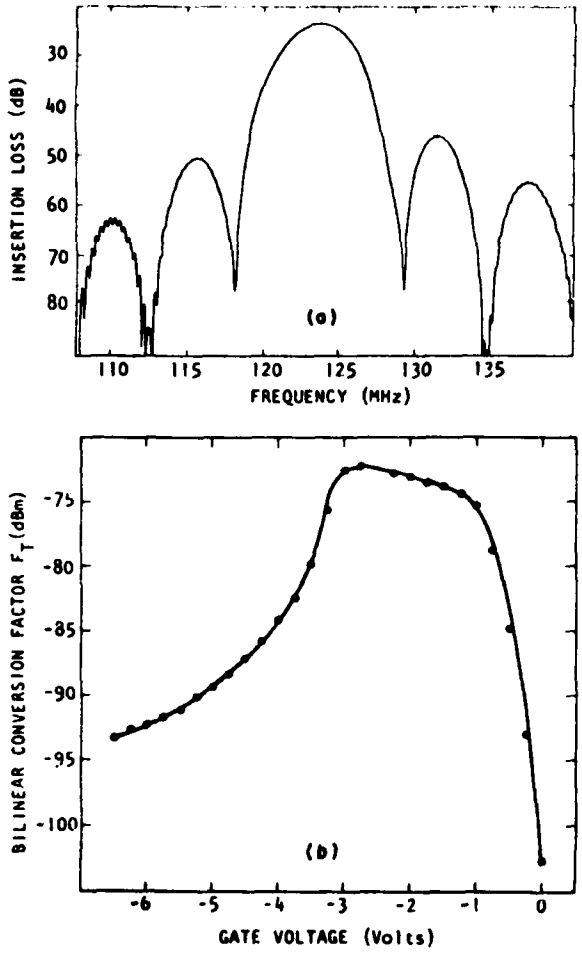

Fig.3.(a) Two-port insertion loss versus frequency and (b) convolution bilinear conversion efficiency (F_T) versus gate bias obtained from an N_2 annealed convolver. Transducers were d.c. biased so as to accumulate the underlying silicon surfaces.

point on the F_T versus V_G curve within seconds after a change is made in the d.c. bias applied to the convolver gate.

The improvement in bias stability resulting from the post-sputtering anneal is perhaps best illustrated by referring to the capacitance-voltage ($C\text{-}V_G$) characteristics displayed in Figures 4a and 4b. All curves were

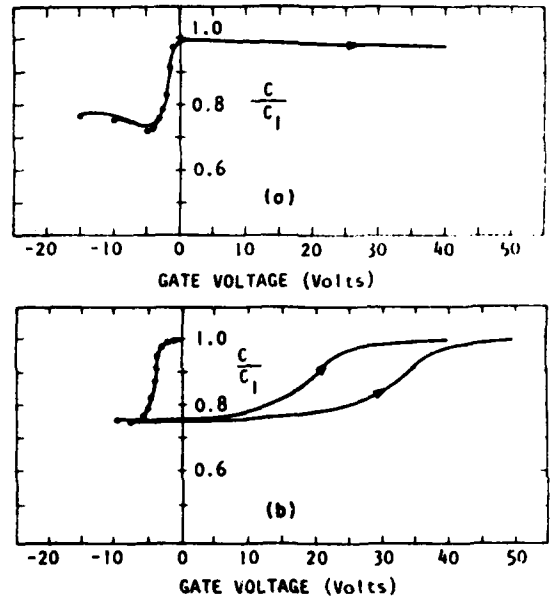

Fig.4.Capacitance-voltage characteristics obtained from (a) an N_2 annealed MZOS capacitor and (b) a similarly fabricated non-annealed capacitor. Stationary $C\text{-}V_G$ characteristics are indicated by dots. The positively swept curves were recorded at 2.5 V/sec starting from heavy inversion.

obtained from test devices probed in a light-tight darkbox. In each case the gate voltage was first stepped negatively in small increments and stationary characteristics (the dots in Figs. 4a and 4b) were recorded. Next the gate voltage was swept positively at 2.5 V/sec from various inversion points. Figure 4a is typical of the $C\text{-}V_G$ characteristics obtained from MZOS capacitors on N_2 annealed test structures. Inspection reveals the positively swept curves are essentially coincident with the $C\text{-}V_G$ data obtained by stepping negatively from V_G=0. By way of comparison, Fig. 4b was derived from a similarly constructed and probed MZOS capacitor which had not been annealed. The large translation in the positively-swept characteristic in Fig. 4b (similar to that displayed earlier in Fig. 1) is typical of non-annealed devices and complete relaxation in this case takes hours to days.

Discussion

Although the aforementioned results are repeatable, it must be acknowledged that the nature of the as-sputtered ZnO film plays a major role in the success of the subsequent annealing procedure. Specifically, the

charge trapping characteristics of rf diode sputtered (non-magnetron) ZnO films produced in our laboratory are essentially unaffected by annealing at 380 °C - 485 °C in an N_2 atmosphere. Investigating this negative result, however, has had the positive effect of providing insight into the bias stability of the annealed magnetron sputtered films. Extensive measurements of the a.c. conductance of MZOS capacitors incorporating differently processed ZnO films has revealed a fundamental difference in the conduction mechanism operating within the films. The room temperature a.c. conductivity of magnetron sputtered films always exhibits a dominant hopping [9] component which is enhanced by thermal annealing. In rf diode films, on the other hand, hopping conduction is not observed. Based on the admittance observations, then, we are led to speculate that charge can be injected and extracted from the ZnO-SiO_2 interfacial region of magnetron sputtered structures via a charge hopping mechanism; ie., as pictured in Fig. 5, deep level traps

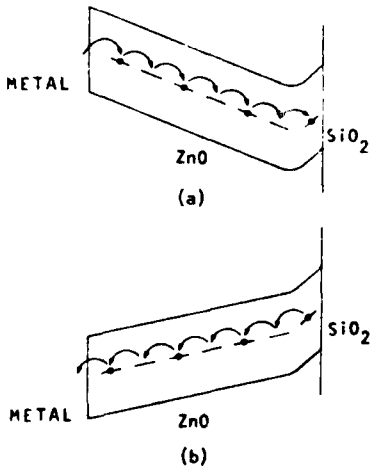

Fig.5.Model for (a) charge injection and (b) charge extraction in annealed MZOS structures.

can communicate directly in transfering charge to and from the ZnO-SiO_2 interface. Moreover, thermal annealing of the magnetron sputtered films is assumed to increase the concentration of centers required for hopping, thereby facilitating a more rapid transport of charge. Whether the increased hopping center concentration is caused by a dispersal of impurity conglomerates, a propagation of defects, or has some other origin is open to conjecture. A comparative physical evaluation of the ZnO films has, in fact, been undertaken to clarify the situation.

Finally, a comment is in order concerning the absence of transducer underlays in the test devices. If underlays are used they will, of course, be in place during the anneal. Following annealing, magnetron sputtered ZnO films over underlays have been found to be highly conductive, presumably due to the incorporation of aluminum into the ZnO layer [10]. Likewise, gold underlays were visibly degraded after a 60 minute anneal at 490 °C. Omission of the underlayer actually had little effect on the performance of the test devices. Device performance was optimized by simply applying a small d.c. bias to the transducers so as to heavily accumulate the underlying silicon surface.

Conclusion

ZnO-on-Si SAW devices have been constructed which rapidly attain a repeatable d.c. operating point after both negative and positive changes in gate bias. This bias stability is achieved by annealing magnetron sputtered ZnO films for 60 minutes in a nitrogen atmosphere at temperatures ranging from 380 °C to 490 °C. The thermal anneal is believed to enhance hopping-related charge transport to and from the ZnO-SiO_2 interface. Continuing investigations are being performed to optimize the annealing process and to clarify the physical effects of the anneal.

Acknowledgement

This work was supported by the National Science Foundation under grant ECS-8009793 and the Air Force Office of Scientific Research under grant AFOSR-77-3304.

References

[1] L. A. Coldren, "Effect of Bias Field in a Zinc Oxide-on-Silicon Acoustic Convolver", *Appl. Phys. Lett.*, vol. 25, pp. 473-475, November 1974.

[2] K. L. Davis, "Properties of the MZOS Surface Wave Convolver Configuration", *IEEE Trans. Electron Devices*, vol. ED-23, pp. 554-559, June 1976.

[3] R. F. Pierret, R. L. Gunshor and M. E. Cornell, "Charge Injection in Metal-ZnO-SiO_2-Si Structures", *J. Appl. Phys.*, vol. 50, pp. 8112-8124, December 1979.

[4] H. C. Tuan, J. E. Bowers and G. S. Kino, "Theoretical and Experimental Results for Monolithic SAW Memory Correlators", *IEEE Trans. Sonics and Ultrasonics*, vol. SU-27, pp. 360-369, November 1980.

[5] G. S. Kino, "Zinc Oxide on Silicon Acoustoelectric Devices", *1979 Ultrasonics Symp. Proc.*, pp. 900-910.

[6] B. T. Khuri-Yakub and G. S. Kino, "A Monolithic Zinc Oxide-on-Silicon Convolver", *Appl. Phys. Lett.*, vol. 25, pp. 188-190, August 1974.

[7] K. L. Davis, "Storage of Optical Patterns in a Zinc Oxide-on-Silicon Surface Wave Convolver", *Appl. Phys. Lett.*, vol. 26, pp. 143-145, February 1975.

[8] J. K. Elliott, R. L. Gunshor, R. F. Pierret and K. L. Davis, "Zinc Oxide-Silicon Monolithic Acoustic Surface Wave Optical Image Scanner", *Appl. Phys. Lett.*, vol. 27, pp. 179-182, August 1975.

[9] For a discussion of hopping conduction see N. F. Mott and E. A. Davis, *Electronic Processes in Non-Crystalline Materials*, Second Edition, Oxford University Press, 1979.

[10] T. Hada, K. Wasa and S. Hayakawa, "Structures and Electrical Properties of Zinc Oxide Films Prepared by Low Pressure Sputtering System". *Thin Solid Films*, vol. 7, pp. 135-145, 1971.

Induced junction monolithic zinc oxide-on-silicon storage correlator

K. C. -K. Weng, R. L. Gunshor, and R. F. Pierret
School of Electrical Engineering, Purdue University, West Lafayette, Indiana 47907

(Received 10 August 1981; accepted for publication 9 October 1981)

An induced junction array is proposed as an alternative to the conventional *PN* diode configuration in the implementation of reference storage in a surface acoustic wave SAW storage correlator. Induced junction devices fabricated in the ZnO-on-Si structure are found to exhibit performance characteristics comparable to those of *PN* diode correlators, while providing greater ease of fabrication.

PACS numbers: 43.60. + d, 72.50. + b, 73.40.Qv

The silicon storage (memory) correlator is one of the more promising surface acoustic wave (SAW) devices under consideration for use in real-time signal processing systems. Several physical configurations and reference storage mechanisms have been proposed and investigated in relationship to this device.[1-5] Although signal storage is possible by means of surface states at the SiO_2-Si interface, the most attractive of the configurations employ Schottky or *PN* diode arrays to implement the memory function. In this letter we describe and demonstrate an alternative storage array for use as a SAW correlator, an array consisting of induced junctions.

The proposed device, an adaptation of the metal-ZnO-SiO_2-Si (MZOS) configuration, is shown schematically in Fig. 1. The key feature of the Fig. 1 device is the aluminum grating at the ZnO-SiO_2 interface. As will be explained, the presence of the grating permits the otherwise undesirable charge injection phenomenon, a phenomenon routinely associated with the MZOS structure,[6] to be employed constructively to create the signal storage medium. The interface aluminum grating is fabricated by etching a photoresist-defined Al film depostied over the SiO_2 layer. The Al grating has a periodic spacing of 10 μm and a mark-space ratio of unity. The SiO_2 layer is thermally grown on a 10-Ω cm (100) *n*-type silicon wafer. A phosphorous diffusion step preceeding the Al deposition is used to stabilize the SiO_2 film, getter the Si bulk, and facilitate the formation of an ohmic back contact on the silicon wafer. A 1.6-μm-thick piezoelectric ZnO film is deposited onto the Al grating/SiO_2/Si substrate by means of rf sputtering. The top metalization is designed to minimize spurious response and consists of a dual-track gate together with a pair of symmetric and antisymmetric tansducers[7] fabricated by a photolithographic lift-off procedure. The transducer wavelength is 35.6 μm; the acoustic aperture is 1 mm.

Under operational conditions the center combs of the device are grounded, the antisymmetric and symmetric transducers are driven by a balanced transformer and a two-way 0° power splitter, respectively. With the Al grating grounded, and the device operated as a SAW delay line, one

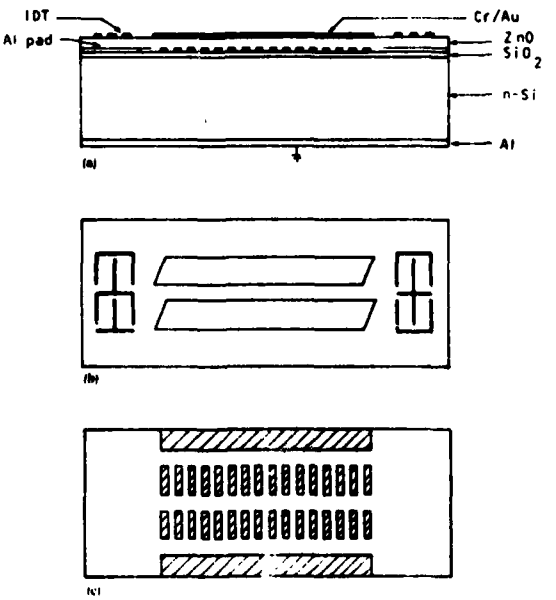

FIG. 1. Schematic of the induced junction correlator. (a) layer structure, (b) top metalization; (c) ZnO/SiO_2 interface Al grating.

 0003-6951/82/010071-03$01.00

observers a 3-dB bandwidth of 7 MHz and an insertion loss of 20 dB at the 18-MHz center frequency. When operated as a degenerate convolver, the device provides an external convolver efficiency of -67 dBm.

Storage correlator operation is achieved by means of an array of isolated induced-junction charge-storage regions. The induced junction array is created by taking advantage of the charge injection phenomena which produces the bias instability found in conventional MZOS devices. Upon application of a negative bias to the gate, electrons are injected into the ZnO layer and either collect on the Al grating or become localized in deep level traps at the ZnO-SiO_2 interface.[6] This initialization step causes an overall inversion of the n-type silicon surface. Following a subsequent positive change in gate bias, the injected charges located on the metal grating are rapidly withdrawn from the interior of the structure. However, in the open regions between the Al grating strips the injected charge is stored in deep level traps for a relatively long period of time (hours or days). The net result of the selective charge removal is an array of induced junction regions where minority carriers are stored in an inversion layer isolated from the silicon bulk. The regions of minority-carrier storage are isolated from each other by depletion regions under the Al grating strips.

The induced junction storage correlator can be operated in any mode suitable for conventional ZnO-on-Si PN diode devices. The specific correlation experiment to be reported herein can be described as follows. The writing process is achieved by applying the rf reference (writing) signal V_w to the gate in coincidence with a narrow acoustic pulse P_a propagating under the gate. The simultaneous presence at the silicon surface of the rf reference signal and the electric field associated with the acoustic signal produces a resultant electric field component normal to the silicon surface. This electric field component (arising from the interaction between the reference signal and the narrow acoustic pulse) in turn causes a measured fraction of the minority carriers to be injected from the iversion layer into the interior of the semiconductor where they recombine. The resultant deficit of the minority carriers within the induced junction array permits the reference signal to be stored as a spatially varying charge pattern at the silicon surface. After a preselected time interval, an rf reading signal V_r is applied to the gate. The nonlinear interaction between the reading signal and the reference signal stored in the induced junction array excites a surface acoustic wave whose envelope represents the correlation output. Employing the aforedescribed mode of operation, a maximum correlation efficiency[8] of -66 dBm has been obtained. The autocorrelation of a stored 5-bit Barker code waveform is shown in Fig. 2(a) (some electromagnetic coupled response also appears at the left in this figure); Fig. 2(b) shows the autocorrelation of two rectangular pulses. The reference signals are written with a 200-ns acoustic pulse.

The dynamic range of the induced junction device is limited for the most part by the degree of energy-band bending within the silicon established during the initialization procedure. At sufficiently high signal levels the rf potential at the silicon surface can become large enough to negate the band bending and allow bulk majority carriers into the near-

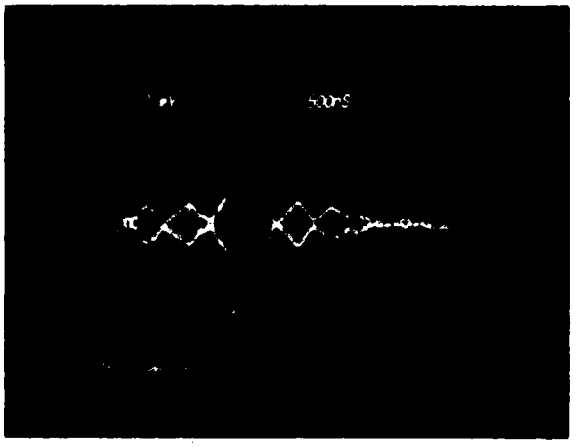

(a)

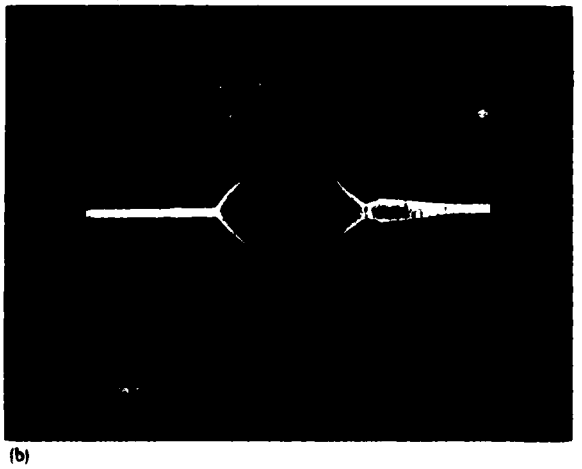

(b)

FIG. 2. Autocorrelation outputs of (a) 5-bit Barker code and (b) two rectangular pulses.

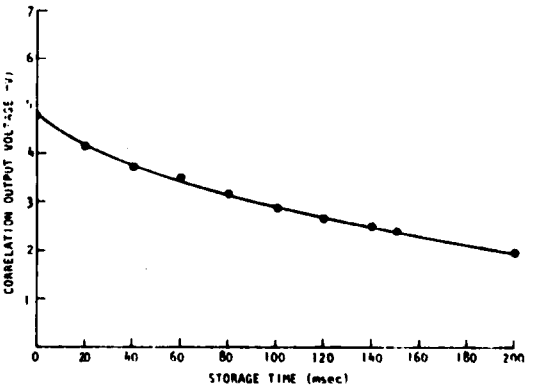

FIG. 3. Correlation output voltage vs storage time ($P_a = 28$ dBm, $T_a = 200$ ns; $V_w = 2$ V, $T_w = 4\,\mu$s; $V_r = 1$ V, $T_r = 4\,\mu$s).

surface region, thereby causing the minority carriers to be annihilated at an accelerated rate through recombination. The result is a rapid loss of the stored reference signal. Experimentally, by varying the writing signal we have observed an input dynamic range of 31 dB, corresponding to a maximum power of 28 dBm for the narrow acoustic pulse and a 10-V peak-to-peak gate signal for read-out. The output dynamic range, determined at an input acoustic power of 28 dBm and with an 8.5-V peak-to-peak gate voltage for write-in, is 40 dB.

The characteristic decay constant τ of the stored signal depends upon the relaxation process of the nonequilibrium condition created within the semiconductor when a charge deficit is produced by the write-in process. To a first-order approximation, the decay constant can be expressed as[9]

$$\tau = 2\tau_0 N_D / n_i,$$

when τ_0 is the generation lifetime, N_D is the semiconductor doping constant, and n_i is the intrinsic carrier concentration. The measured variation of correlator output with storage time is shown in Fig. 3. The observed decay constant is 0.2 s, corresponding to a generation lifetime on the order of tens of microseconds. The time at which the correlation output decays to 3 dB of maximum is 80 ms.

When compared to conventional ZnO-on-Si diode storage correlators, the induced junction configuration exhibits comparable maximum correlation efficiencies[8] and dynamic range.[4,8] In addition, the signal storage time is of the same order of magnitude for both induced junction and diode storage correlators. A more careful fabrication scheme aimed at increasing the minority-carrier lifetime could extend the storage time to tens of seconds.

To summarize, we have described a new type of monolithic ZnO-on-Si storage correlator in which the *PN* diodes are replaced by a more easily fabricated induced junction array. The observed device characteristics are similar to those of diode correlators, while providing opportunities for use in conjunction with semiconductors other than silicon.

The research was supported by the Air Force Office of Scientific Research under grant AFOSR-77-3304 and NSF grant No. ECS-810-744.

[1]A. Bers and J. H. Cafarella, Appl. Phys. Lett. **25**, 133 (1974).
[2]K. A. Ingebrigtsen, R. A. Cohen, and R. W. Mountain, Appl. Phys. Lett. **26**, 596 (1975).
[3]H. C. Tuan and G. S. Kino, Appl. Phys. Lett. **31**, 641 (1977).
[4]F. C. Lo, R. L. Gunshor, and R. F. Pierret, Appl. Phys. Lett. **34**, 725 (1979).
[5]F. C. Lo, R. L. Gunshor, R. F. Pierret, and J. K. Elliott, Appl. Phys. Lett. **33**, 903 (1978).
[6]R. F. Pierret, R. L. Gunshor, and M. E. Cornell, J. Appl. Phys. **50**, 8112 (1979).
[7]I. Yao, *1980 Ultrasonics Symposium Proceeding*, IEEE Cat. No. 80CH1602-2 (IEEE, New York, 1980).
[8]H. C. Tuan, J. E. Bowers, and G. S. Kino, IEEE Trans. Sonics Ultrason. **SU-27**, 360 (1980).
[9]F. P. Heiman, IEEE Trans. Electron. Devices **ED-14**, 781 (1967).


DATE
ILME